

RESEARCH PAPER

Nitrogen metabolism of two contrasting poplar species during acclimation to limiting nitrogen availability

Jie Luo¹, Hong Li², Tongxian Liu², Andrea Polle³, Changhui Peng⁴ and Zhi-Bin Luo^{1,4,*}¹ College of Life Sciences and State Key Laboratory of Crop Stress Biology in Arid Areas, Northwest A&F University, Yangling, Shaanxi 712100, PR China² Key Laboratory of Applied Entomology, College of Plant Protection, Northwest A&F University, Yangling, Shaanxi 712100, PR China³ Büsgen-Institute, Department of Forest Botany and Tree Physiology, Georg-August University, Büsgenweg 2, 37077 Göttingen, Germany⁴ Key Laboratory of Environment and Ecology in Western China of Ministry of Education, College of Forestry, Northwest A&F University, Yangling, Shaanxi 712100, PR China* To whom correspondence should be addressed. E-mail: luozbbill@163.com

Received 25 April 2013; Revised 11 June 2013; Accepted 25 June 2013

Abstract

To investigate N metabolism of two contrasting *Populus* species in acclimation to low N availability, saplings of slow-growing species (*Populus popularis*, Pp) and a fast-growing species (*Populus alba* × *Populus glandulosa*, Pg) were exposed to 10, 100, or 1000 μM NH₄NO₃. Despite greater root biomass and fine root surface area in Pp, lower net influxes of NH₄⁺ and NO₃⁻ at the root surface were detected in Pp compared to those in Pg, corresponding well to lower NH₄⁺ and NO₃⁻ content and total N concentration in Pp roots. Meanwhile, higher stable N isotope composition (δ¹⁵N) in roots and stronger responsiveness of transcriptional regulation of 18 genes involved in N metabolism were found in roots and leaves of Pp compared to those of Pg. These results indicate that the N metabolism of Pp is more sensitive to decreasing N availability than that of Pg. In both species, low N treatments decreased net influxes of NH₄⁺ and NO₃⁻, root NH₄⁺ and foliar NO₃⁻ content, root NR activities, total N concentration in roots and leaves, and transcript levels of most ammonium (*AMTs*) and nitrate (*NRTs*) transporter genes in leaves and genes involved in N assimilation in roots and leaves. Low N availability increased fine root surface area, foliar starch concentration, δ¹⁵N in roots and leaves, and transcript abundance of several *AMTs* (e.g. *AMT1;2*) and *NRTs* (e.g. *NRT1;2* and *NRT2;4B*) in roots of both species. These data indicate that poplar species slow down processes of N acquisition and assimilation in acclimation to limiting N supply.

Key words: Gene expression, glutamate synthase, glutamine synthetase, net flux, nitrate reductase, nitrite reductase, plasma membrane H⁺-ATPase, poplar, stable carbon isotope.

Introduction

As woody crops, forest plantations hold a great potential for the pulp and paper industry, carbon mitigation, and biomass production for biofuels (Luo *et al.*, 2006; Luo and Polle, 2009; Novaes *et al.*, 2009; Studer *et al.*, 2011). Plantations of some fast-growing tree species such as *Populus* spp. have been widely established in recent years (Weih, 2004; Polle and Douglas, 2010; Rennenberg *et al.*, 2010). As a riparian species,

Populus in its natural habitat is supplied with sufficient nitrogen (N) derived from intensive N-fertilization application in agriculture (Rennenberg *et al.*, 2010; Koyama and Kielland, 2011). Due to the high demand of fertile soil for agriculture, however, poplar plantations have often been established on marginal lands where soil N is limiting (Rennenberg *et al.*, 2010; Bilodeau-Gauthier *et al.*, 2011). In this context, it is of

particular importance to select poplar species with tolerance to low N availability.

The genus *Populus* contains about 30–40 species which may differ in N metabolism (Calfapietra *et al.*, 2007; Finzi *et al.*, 2007; Euring *et al.*, 2012; Li *et al.*, 2012). For instance, *Populus tremula* × *Populus tremuloides* is a species that often occurs on nutrient-poor soil. The growth and wood properties of this species are more responsive to different N levels than those of *Populus trichocarpa* which is adapted to fluctuating N supply (Euring *et al.*, 2012). These results highlight that it is essential to better understand the distinctness of N metabolism in different poplar species in order to select poplars with tolerance to low N availability.

Although little information is available on responses of N metabolism in different woody plants to low N availability, distinct N metabolism has been reported in different herbaceous species or genotypes in response to N deficiency (Lawlor *et al.*, 1987a, 1988, 1989; Lawlor, 2002; Hirel *et al.*, 2007; Shen *et al.*, 2013). For instance, some maize varieties displayed a higher capacity to absorb and utilize N than the others (Banziger *et al.*, 1997; Toledo Machado and Silvestre Fernandes, 2001). In cereal crops, earlier studies demonstrated that N deficiency in soil often led to altered root length and branching and decreased soluble protein concentration and photosynthetic activity (Maizlich *et al.*, 1980; Lawlor *et al.*, 1987b, 1989; Lawlor, 2002; Hirel *et al.*, 2007). Plants with tolerance to low N are often associated with higher photosynthetic N use efficiency (PNUE), greater root length, and surface area per volume of soil (Lawlor, 2002; Hirel *et al.*, 2007; Shen *et al.*, 2013). However, the physiological and molecular mechanisms remain to be elucidated for plant species differing in tolerance to low N supply.

In plants, the N metabolism process involves uptake, transport, assimilation, and utilization for amino acid biosynthesis and ultimately for growth (Nunes-Nesi *et al.*, 2010). Each of these steps may be regulated slightly different, leading to differences in N metabolism and performance of plants with distinct ecological requirements. In herbaceous plants, the N metabolism processes are well documented (Fig. 1), which may serve as a conceptual model to address N metabolism of different poplar species in response to low N availability.

In the N uptake process, NH_4^+ and nitrate NO_3^- in soil solution are the two major inorganic N forms for plant absorption. Although both ions can be used by plants, the energetic, biochemical, and molecular features of NH_4^+ and NO_3^- are different for metabolism, leading to distinct net fluxes of both ions at the root surfaces and NH_4^+ or NO_3^- preference of plants (Jackson *et al.*, 2008; Patterson *et al.*, 2010). Using ^{15}N labelling, it was demonstrated that some woody plants prefer NH_4^+ (Rennenberg *et al.*, 2009, 2010). Additionally, net fluxes of NH_4^+ and/or NO_3^- at the root surfaces have been investigated using ion-selective microelectrodes in herbaceous and woody plants (Plassard *et al.*, 2002; Gobert and Plassard, 2007; Hawkins *et al.*, 2008; Hawkins and Robbins, 2010; Alber *et al.*, 2012; Luo *et al.*, 2013), providing a better understanding of electrophysiological processes of NH_4^+ and NO_3^- acquisition. The net fluxes of both NH_4^+ and NO_3^- are coupled with the activities of plasma membrane (PM)

H^+ -ATPases in fine roots of *Populus popularis* (Luo *et al.*, 2013). However, comparisons of fluxes of NH_4^+ and NO_3^- at the root surface of poplar species with large differences in growth are missing.

The fluxes of NH_4^+ and NO_3^- are mediated by various transporters for ammonium (AMTs) and nitrate (NRTs) (Rennenberg *et al.*, 2010; Xu *et al.*, 2012). Some AMTs and NRTs have been functionally elucidated in *Arabidopsis thaliana* (Wang *et al.*, 2012; Xu *et al.*, 2012). For instance, transcript abundance of *AtAMT1;1* is strongly increased by N starvation and reduced upon NH_4^+ supply in *Arabidopsis* roots (Engelsberger and Schulze, 2012). Some NRT members such as AtNRT1;1, AtNRT1;2, AtNRT2;1, and AtNRT3;1 play pivotal roles in NO_3^- uptake and signalling (Yong *et al.*, 2010; Kotur *et al.*, 2012; Wang *et al.*, 2012). In the genome of *P. trichocarpa*, 14 putative AMTs have been documented (Tuskan *et al.*, 2006; Couturier *et al.*, 2007), whereas less is known about the NRT members (Plett *et al.*, 2010; Rennenberg *et al.*, 2010; Li *et al.*, 2012). Several studies showed that transcripts of putative poplar transporters (e.g. AMT1;2, AMT1;6, AMT2;1, NRT1;1, NRT1;2, NRT2;4B, NRT2;4C, NRT3.1B, and NRT3.1C) were responsive to environmental fluctuations under non-limiting N conditions (Selle *et al.*, 2005; Couturier *et al.*, 2007; Dluzniewska *et al.*, 2007; Ehltling *et al.*, 2007; Plett *et al.*, 2010; Li *et al.*, 2012). However, it remains unknown how transcriptional regulation of these transporters responds to limiting N supply in different poplar species.

After uptake into the roots, a large amount of NH_4^+ can be assimilated locally and the remainder is translocated to leaves or other parts of the plant, whereas only a limited amount of NO_3^- is assimilated in roots and most NO_3^- is transported to leaves (Black *et al.*, 2002; Xu *et al.*, 2012). In the assimilation process, NO_3^- is converted to NH_4^+ by nitrate reductase (NR) and nitrite reductase (NiR) (Xu *et al.*, 2012). Subsequently, NH_4^+ can be assimilated to glutamine catalysed by glutamine synthetase (GS) (Castro-Rodriguez *et al.*, 2011; Coleman *et al.*, 2012). The formation of glutamate requires glutamine and 2-oxoglutarate in a reaction catalysed by glutamate synthase (GOGAT) (McAllister *et al.*, 2012). Additionally, glutamate can be synthesized by glutamate dehydrogenase (GDH) under consumption of NH_4^+ and 2-oxoglutarate (McAllister *et al.*, 2012). Very little is known about the response of these enzymes to low N supply in different poplar species.

Although forest plantations often grow on nutrient-poor soils (Johnson, 2006; Rennenberg *et al.*, 2009), N-related studies in trees mainly addressed the effects of fertilization but less to uncover the responses to N-limitation (Cooke and Weih, 2005; Rennenberg *et al.*, 2009, 2010; Lukac *et al.*, 2010; Millard and Grelet, 2010). Recently, we found that growth, carbon, and N physiology, and wood properties of the fast-growing *Populus alba* × *Populus glandulosa* (Pg), which generally grows on relatively fertile soils, displays a stronger responsiveness to N-fertilization than the slow-growing *P. popularis* (Pp) which is often found on nutrient-deficient soils (Li *et al.*, 2012). The differential responses are ascribed to prioritized resource allocation to the leaves and accelerated N physiological processes in the fast-growing Pg under

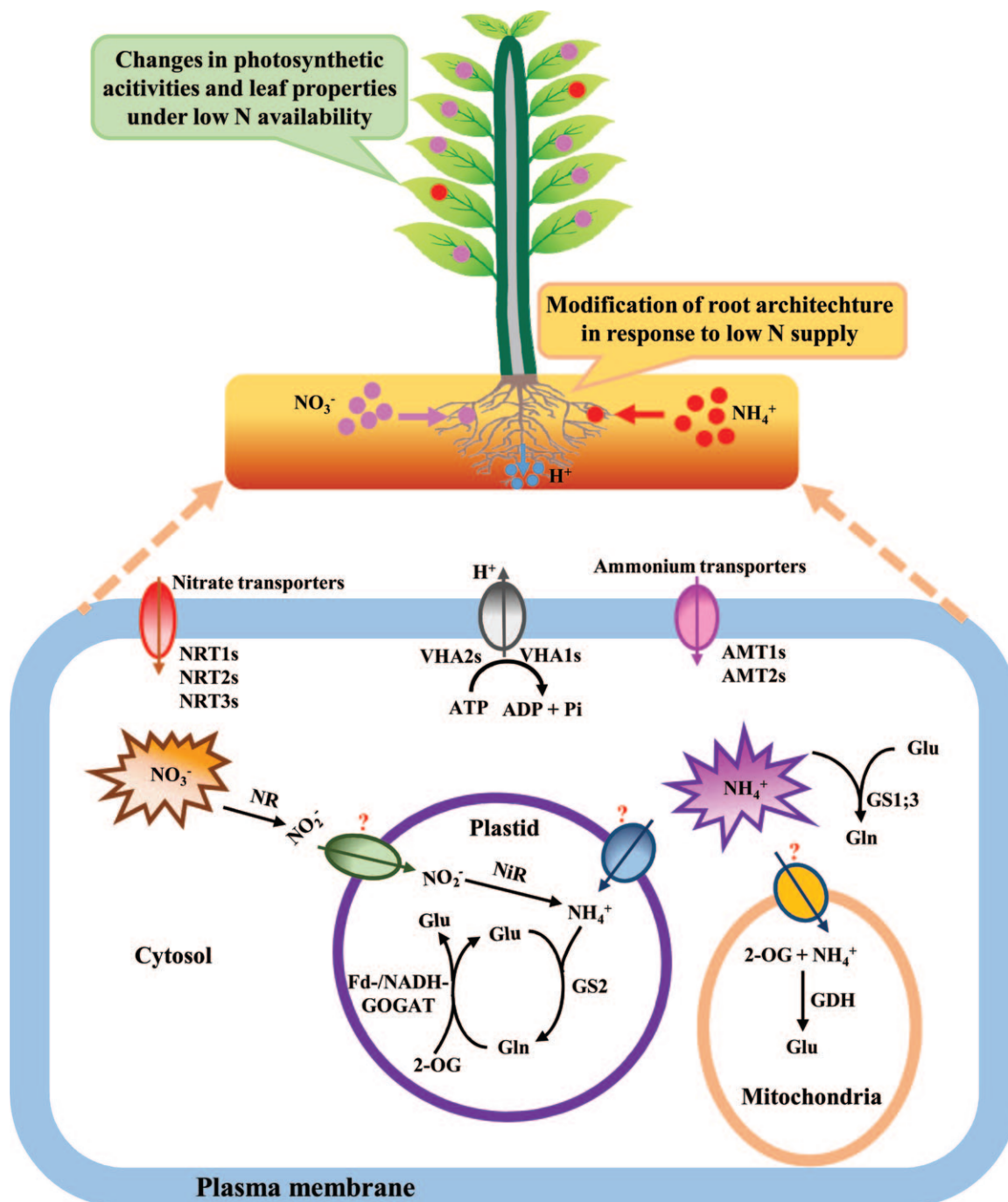


Fig. 1. A conceptual model of N metabolism in plants. In the uptake process, NH_4^+ and NO_3^- enter the cytosol via ammonium (AMTs) and nitrate (NRTs) transporters, respectively, coupled with plasma membrane H^+ -ATPases (VHAs). After uptake in roots, NH_4^+ and NO_3^- can be translocated to leaves or other parts of the plant. In the assimilation process, NO_3^- is converted to NH_4^+ by the cytosolic nitrate reductase (NR) and the plastidic/chloroplastic nitrite reductase (NiR). Subsequently, NH_4^+ can be assimilated to glutamine (Gln) catalysed by glutamine synthetase (GS) isoenzymes either in the plastid or the cytosol. The Gln in the plastid with 2-oxoglutarate (2-OG) can be further converted to glutamate (Glu) by Fd- or NADH-dependent glutamate synthase (Fd/NADH-GOGAT). Additionally, in the mitochondrion, NH_4^+ can be assimilated to Glu with glutamate dehydrogenase (GDH). The synthesized N compounds provide precursors for amino acids, proteins, and other N-containing metabolites which can be utilized by plant growth. At the cellular level, N metabolism in plants can be affected by external low N availability. At the plant level, root characteristics, photosynthetic activity, and leaf properties can be altered in response to low N supply (this figure is available in colour at *JXB* online).

higher N supply levels. However, it remains unknown how N metabolism processes and key components involved in these processes of Pp and Pg respond to external low N availability.

This study exposed Pp and Pg to low N levels. Measurements of morphological (root characteristics), physiological (e.g. photosynthesis, net fluxes of NH_4^+ , NO_3^- , and H^+ ,

accumulation of NH_4^+ , NO_3^- , and NO_2^- , total N concentration, and $\delta^{15}\text{N}$), and molecular (transcript levels of representative genes involved in N metabolism) parameters known to be important for acclimation to low N availability were conducted. Furthermore, multivariate analysis was applied to dissect the importance of parameters as contributors to the acclimation of N metabolism in both poplar species to low N supply. The following questions were specifically addressed: (i) do root morphology, photosynthesis, and N metabolism of Pp and Pg display different response patterns to limiting N supply? and (ii) what are the physiological and transcriptional regulation mechanisms of Pp and Pg in acclimation to low N availability?

Materials and methods

Plant cultivation and N treatment

Cuttings of the slow-growing *P. popularis* (Pp) and the fast-growing *P. alba* × *P. glandulosa* (Pg) were rooted as described previously (Li *et al.*, 2012), and planted in pots (10 l) filled with fine sand. Plants were cultivated in a greenhouse (natural light, day/night 25/20 °C, 75% relative humidity) and provided with 50 ml Long Ashton (LA) nutrient solution, which contains 1000 μM NH_4NO_3 (Dluzniewska *et al.*, 2007) every other day. After 6 weeks, plants with similar height (*c.* 60 cm) were selected for further study. The root systems of selected plants were carefully washed with tap water. Plants of each species were divided into three groups with 18 plants for each group. Subsequently, plants of three groups from each species were cultivated in hydroponics with modified LA solution (0.5 mM KCl, 0.9 mM CaCl_2 , 0.3 mM MgSO_4 , 0.6 mM KH_2PO_4 , 42 μM K_2HPO_4 , 10 μM Fe-EDTA, 2 μM MnSO_4 , 10 μM H_3BO_3 , 7 μM Na_2MoO_4 , 0.05 μM CoSO_4 , 0.2 μM ZnSO_4 , and 0.2 μM CuSO_4) containing 10, 100, or 1000 μM NH_4NO_3 , respectively, and the nutrient solution was adjusted to pH 5.5. The LA solution was refreshed every 2 days. In the greenhouse, the position of each plant was randomly assigned and altered once a week. At the beginning of the N treatment, the apex of each plant was marked by using a laboratory marker to distinguish the shoots formed during the N treatment. After hydroponic cultivation with N treatments for 3 weeks from 20 June to 10 July, 12 plants of each group were used for gas exchange determination prior to harvest and the remaining six plants of each group were used for measurements of net fluxes of NH_4^+ and NO_3^- .

Gas exchange and harvesting

The gas exchange of three mature leaves (leaf plastochron index = 8–10) formed during N treatment was determined for each plant. Net photosynthetic rates (*A*), stomatal conductance (g_s), and transpiration rates were determined with a portable photosynthesis system (Li-Cor-6400, Li-Cor, Lincoln, NE, USA) and an attached LED light source (6400-02) as described by He *et al.* (2011). The instantaneous photosynthetic N use efficiency (PNUE_i) was calculated based on *A*, foliar N concentration, and specific leaf area, as suggested by Li *et al.* (2012). As a stored photosynthate, starch concentration in harvested root and leaf tissues (see below) was analysed as suggested by He *et al.* (2013).

Since the daily rhythm of plants can affect physiological and molecular processes (Wilkins *et al.*, 2009), the harvest was performed between 9:00 and 12:00. For harvest, the root system of each plant was well washed with corresponding LA solution containing 10, 100, or 1000 μM NH_4NO_3 . Subsequently, the root system was wrapped in lab tissue paper to remove water on the root surface. Length of main root and fresh weight of roots were recorded. A part of roots (*c.* 2 g) of each plant was excised from the root system, scanned, and analysed by a WinRHIZO root analyser system

(WinRHIZO version 2012b, Regent Instruments Canada, Montreal, Canada) as described by Luo *et al.* (2013). Leaves formed during the N treatment (above the mark on the stem) were harvested. Leaf discs for determination of specific leaf area were also collected and specific leaf area was calculated according to the method of Cao *et al.* (2012). Harvested roots or leaves were wrapped with tinfoil and immediately frozen in liquid N. Root or leaf samples were ground into fine powder in liquid N with a mortar and pestle and stored at -80 °C. Frozen powder (*c.* 100 mg) from roots or leaves of each plant was dried at 60 °C for 72 h to determine the fresh-to-dry-mass ratio. For further biochemical analysis, equal weight of fine powder from roots or leaves of two plants within each group was combined to form a well-mixed sample.

Analysis of net fluxes of NH_4^+ , NO_3^- , and H^+

To analyse net fluxes of NH_4^+ , NO_3^- , and H^+ at the root surface, three white fine roots (*c.* 1.5 mm in diameter) were randomly selected from the root system of each plant. Net fluxes of these ions were measured non-invasively using scanning ion-selective electrode technique (SIET, SIET system BIO-003A, Younger USA Science and Technology, Falmouth, MA, USA) by Xuyue Science and Technology (Beijing, China). The SIET system and its application in net ion flux detection were described in detail (Li *et al.*, 2010; He *et al.*, 2011; Luo *et al.*, 2013). The ion-selective microelectrode with 2–4 μm aperture was manufactured and silanized with a backfilling solution and an ion-selective liquid cocktail.

To find out the positions along the root where the maximal net fluxes of NH_4^+ and NO_3^- take place, a preliminary experiment was performed using plants treated with 100 μM NH_4NO_3 by taking an initial measurement at the root apex, followed by measurements at 300 μm intervals (in the region of 0–2100 μm) or 5 mm intervals (in the region of 5–30 mm) along the root tip (Supplementary Fig. S1A, available at JXB online). Ion gradients near the root surface were measured by moving the ion-selective microelectrode between two positions (*c.* 30 μm in distance) in a perpendicular direction to the root axis. The recording rate for these ion fluxes was one reading per 6 s and ion flux was recorded at each measurement point for 10 min.

For the positions where the maximal net fluxes of NH_4^+ and NO_3^- occur in roots, net fluxes of NH_4^+ , NO_3^- , and H^+ were further investigated in detail. A fine root was transferred to a Petri dish containing 10 ml measuring solution (0.1 mM KCl, 0.1 mM CaCl_2 , pH 5.5) with 10, 100, or 1000 μM NH_4NO_3 according to the N treatment of the selected root, and equilibrated for 20 min. Prior to the measurement, the root was transferred to a new Petri dish containing fresh measuring solution and net NH_4^+ fluxes were monitored for 10 min. Afterwards, net NO_3^- fluxes were measured for 10 min in the same root and finally, net H^+ fluxes were recorded for 10 min in the root.

Isolation of the PM and measurement of PM H^+ -ATPase activity

PM vesicles of root cells were isolated according to the method of Sorgona *et al.* (2011) with minor modification. Briefly, fine powder of roots (*c.* 2 g) was homogenized with 3 ml extraction solution containing 250 mM sucrose, 10% (v/v) glycerol, 10 mM glycerol-1-phosphate, 2 mM MgSO_4 , 2 mM EDTA, 2 mM EGTA, 2 mM ATP, 2 mM DTT, 5.7% (w/v) choline chloride, 25 mM 1,3-bis(tris(hydroxymethyl)-methyl-aminoethylether)propane (BTP, pH 7.6 with 2(N-morpholino)ethanesulphonic acid, MES), 1 mM PMSF, and 20 $\mu\text{g ml}^{-1}$ chimosatin at 4 °C. After centrifugation (12,700 g, 4 °C, 30 min), the pellets were suspended over a 25/38% discontinuous sucrose gradient (5 mM MES containing all protectants present in the extraction solution, pH 7.4). Afterwards, the gradient was centrifuged again (12,700 g, 4 °C, 60 min). The pellets were resuspended in a medium containing 20% glycerol (v/v), 2 mM EGTA, 2 mM EDTA, 0.5 mM ATP, 1 mM PMSF, 2 mM DTT, 20 $\mu\text{g ml}^{-1}$ chimosatin, 5.7% choline chloride, and 5 mM BTP buffered at pH 7.0 with MES and immediately frozen in liquid N and stored at -80 °C.

PM H⁺-ATPase activity was determined spectrophotometrically at 700 nm as described by [Sorgona et al. \(2011\)](#) with minor modifications. In brief, assays were carried out at 30 °C in 0.5 ml medium containing 30 mM BTP/MES (pH 6.5), 5 mM MgSO₄, 50 mM KCl, 4 mM ATP, 0.6 mM Na₂MoO₄, 100 mM KNO₃, 1.5 mM NaN₃, and 0.02% (w/v) polyoxyethylene 20 cetyl ether, with or without 100 μM vanadate (an inhibitor of P-type H⁺-ATPase). The difference between these two activities was attributed to the PM H⁺-ATPase. Sodium azide and KNO₃ were used as selective inhibitors of mitochondrial and tonoplast H⁺-ATPase, respectively ([Zhu et al., 2009](#)). The reaction was initiated by adding membrane vesicles (5–10 μg membrane protein) and stopped after 30 min with a solution containing 2% (v/v) concentrated H₂SO₄, 5% (w/v) SDS, 0.7% Na₂MoO₄, and 10% ascorbic acid. After solubilizing the membrane vesicles with 0.5 M NaOH ([Gogstad and Krutnes, 1982](#)), the total soluble protein was estimated according to [Bradford \(1976\)](#). PM H⁺-ATPase activity was expressed as that inhibited by 100 μM vanadate.

Determination of NH₄⁺, NO₃⁻, and NO₂⁻ concentration

NH₄⁺ concentration in roots and leaves was determined based on the Berthelot reaction ([Brautigam et al., 2007](#); [Luo et al., 2013](#)). In brief, fine powder (*c.* 100 mg) was homogenized in an extraction solution (1 ml 100 mM HCl and 500 μl chloroform). The extraction solution was centrifuged (10,000 g, 4 °C, 10 min) after shaking for 15 min at 4 °C. The aqueous phase was transferred to a 2 ml tube with 50 mg activated charcoal, mixed well, and centrifuged (12,000 g, 4 °C, 5 min) again. NH₄⁺ concentration in the supernatant was determined spectrophotometrically at 620 nm.

NO₃⁻ concentration in samples was analysed as suggested by [Patterson et al. \(2010\)](#). Fine powder (*c.* 100 mg) was extracted in 1 ml deionized water at 45 °C for 1 h. After centrifugation (5000 g, 20 °C, 15 min), the supernatant was used for nitrate quantification. The supernatant (0.2 ml) was mixed thoroughly with 0.8 ml of 5% (w/v) salicylic acid in concentrated H₂SO₄. After incubation at room temperature for 20 min, 19 ml of 2 M NaOH was added to raise the pH to above 12. The solution was cooled to room temperature before NO₃⁻ concentration was determined spectrophotometrically at 410 nm.

NO₂⁻ concentration in samples was quantified as described by [Ogawa et al. \(1999\)](#). Frozen fine powder (*c.* 100 mg) was extracted by an extraction buffer containing 50 mM TRIS-HCl (pH 7.9), 5 mM cysteine, and 2 mM EDTA. After centrifugation (10,000 g, 20 °C, 20 min), 500 μl supernatant was mixed with 250 μl 1% sulphanimide and 250 μl 0.02% N-(1-naphthyl)-ethylene-diamine dihydrochloride in 3.0 M HCl. NO₂⁻ concentration was quantified spectrophotometrically at 540 nm.

Determination of enzyme activities

Activities of NR (EC 1.7.99.4) and NiR (EC 1.7.2.1) were determined in roots and leaves according to the methods of [Ehltling et al. \(2007\)](#) and [Ogawa et al. \(1999\)](#), respectively. Briefly, frozen powder (*c.* 200 mg) was extracted in an extraction buffer (100 mM HEPES-KOH (pH 7.5), 5 mM Mg-acetate, 5 mM DTT, 1 mM EDTA, 0.5 mM PMSF, 20 mM FAD, 5 mM Na₂MoO₄, 10% (v/v) glycerin, 1% (w/v) polyvinyl pyrrolidone, 0.5% BSA, 0.1% (v/v) Triton X-100, and either 25 mM leupeptine for leaves or 25 mM chymostatin for roots). The crude extract was used for NR and NiR assays.

For NR, the extract was added to the reaction mixture (100 mM HEPES-KOH (pH 7.5), 6.0 mM KNO₃, 6.0 mM EDTA, 0.6 mM NADH, 12 mM FAD, 6 mM Na₂MoO₄, 3 mM DTT, and either 25 mM leupeptine for leaves or 25 mM chymostatin for roots) at 25 °C. The reaction was terminated after 20 min by adding 0.6 M Zn-acetate and 0.25 mM phenazinemetosulphate. NO₂⁻ formation in the solution was determined as in the assay of NO₂⁻ concentration.

For NiR, 500 μl supernatant from NO₂⁻ concentration assay was concentrated with a Amicon Ultra 10K filter (Millipore, Billerica, USA) to reduce nitrate ions. The concentrated supernatant was

mixed with 500 μl solution containing 50 mM TRIS-HCl (pH 7.5), 1 mM cysteine, and 2 mM EDTA. The NiR activity was determined by following the reduction of NO₂⁻ in the assay. The assay solution contained 0.5 mM NaNO₂, 1 mM methyl viologen, and the extract. The reaction was started by adding the reagent (0.12 M Na₂S₂O₄, 0.2 M NaHCO₃), incubated at 30 °C for 60 min, and terminated by vigorous vortex until the colour of the methyl viologen disappeared completely. After adding 1 M Zn-acetate, the mixture was centrifuged (10,000 g, 25 °C, 10 min). The residual NO₂⁻ in the reaction solution was determined as in the assay of NO₂⁻ concentration.

GS (EC 6.3.1.2) activity was analysed spectrophotometrically as proposed by [Wang et al. \(2008\)](#). Frozen fine powder was homogenized at 4 °C in 50 mM TRIS-HCl extraction solution (pH 8.0) containing 2 mM MgCl₂, 2 mM DTT, and 0.4 M sucrose. After centrifugation (15,000 g, 4 °C, 20 min), the supernatant was used for GS activity assay. The assay solution contained 0.35 ml of 40 mM ATP and 0.8 ml of 0.1 M TRIS-HCl buffer (pH 7.4) with 20 mM Na-glutamate, 80 mM MgSO₄, 20 mM cysteine, 2 mM EGTA, and 80 mM NH₂OH. After adding the enzyme extract to the assay solution, the mixture was incubated (37 °C, 30 min) and the incubation was stopped by addition of the reagent (0.37 M FeCl₃, 0.2 M trichloroacetic acid, 0.6 M HCl). After centrifugation (5000 g, 4 °C, 15 min), the absorbance of the supernatant was recorded at 540 nm. GS activity was expressed as 1 μmol γ-glutamyl hydroxamate formed per min.

Activities of GOGAT (EC 1.4.7.1) and GDH (EC 1.4.1.2) were assayed in roots and leaves based on the method of [Lin and Kao \(1996\)](#). Fine powder (*c.* 100 mg) was extracted with 10 mM TRIS-HCl buffer (pH 7.6), 1 mM MgCl₂, 1 mM EDTA, and 1 mM β-mercaptoethanol at 4 °C. After centrifugation (15,000 g, 4 °C, 30 min), the supernatant was used for determination of enzyme activities. The GOGAT assay solution contained 0.2 ml of 20 mM L-glutamine, 25 μl of 0.1 M 2-oxoglutarate, 50 μl of 10 mM KCl, 0.1 ml of 3 mM NADH, and 0.25 ml enzyme extract in a final volume of 1.5 ml made up with 25 mM TRIS-HCl buffer (pH 7.6). After addition of L-glutamine, the decrease in absorbance was recorded spectrophotometrically at 340 nm. The GDH assay mixture contained 0.15 ml of 0.1 M 2-oxoglutarate, 0.15 ml of 1 M NH₄Cl, 0.1 ml of 3 mM NADH, and 0.5 ml of the enzyme extract in a final volume of 1.5 ml made up with 0.2 M TRIS-HCl buffer (pH 8.0). After addition of enzyme extract, the decrease in absorbance was monitored spectrophotometrically at 340 nm.

Determination of total carbon and nitrogen and stable isotopes

Root samples and mature leaves used for gas exchange measurements were harvested for total C and N and stable isotope (¹³C and ¹⁵N) analysis. Total C and N concentration was determined according to the method of [Luo and Polle \(2009\)](#). The stable C isotope (¹³C) was analysed based on the protocol of [Cao et al. \(2012\)](#). Fine powder (*c.* 50 mg) was dried in an oven at 80 °C. The dried powder (*c.* 0.8 mg) was sealed under vacuum in a quartz tube with copper oxide and silver foil and combusted for at least 4 h at 800–850 °C. The CO₂ from the combustion tube was extracted and purified cryogenically. The isotopic ratio of the extracted CO₂ was determined by an elemental analyser (NA 1110, CE Instruments, Rodano, Italy) and a mass spectrometer (Delta Plus, Finnigan MAT, Bremen, Germany) with an interface (ConFlo III, Finnigan MAT, Bremen, Germany) according to the method of [Werner et al. \(1999\)](#). The ¹³C/¹²C ratio is expressed as parts per thousand deviation from the Pee Dee Belemnite standard. Carbon isotope composition (‰) was calculated as δ¹³C = (R_{sa} - R_{sd})/R_{sd} × 1000, where R_{sa} and R_{sd} are the ratios of ¹³C to ¹²C of the sample and the standard, respectively. The standard was referred to CO₂ in air.

Stable N isotope composition (δ¹⁵N) was analysed similarly to ¹³C with minor modifications, according to the method of [Yousfi et al. \(2012\)](#). The standard was referred to N₂ in air.

Determination of mineral nutrients, soluble sugars, soluble protein, and phenolics

Mineral elements in roots and leaves were analysed by an inductively coupled plasma-atomic emission spectrometer (Spectroflame, Spectro Analytical Instruments) based on the protocol of Heinrichs et al. (1986).

Concentrations of total soluble sugar in root and leaf tissues were analysed by the anthrone method of Yemm and Willis (1954) with minor modifications (He et al., 2013). The standard curve was established by using a serial of diluted solutions of glucose. The final absorbance of total soluble sugar and starch (expressed as glucose equivalent) in samples was determined at 620 nm.

Soluble protein in plant materials was extracted and used for quantification (Bradford, 1976). Soluble phenolics were determined according to the method of Swain and Goldstein (1964) with the modification by Luo et al. (2008).

Analysis of transcript levels of genes involved in N uptake and assimilation

The transcriptional changes of genes implicated in N uptake and assimilation were analysed by reverse-transcription quantitative PCR (qPCR) based on the method (Li et al., 2012). Briefly, frozen fine powder of roots (c.100 mg) and leaves (c.50 mg) was used for total RNA isolation. Total RNA was isolated and purified with a plant RNA extraction kit (R6827, Omega Bio-Tek, GA, USA) and trace genomic DNA was digested by DNase I (E1091, Omega Bio-Tek) attached to the RNA extraction kit. The lack of trace genomic DNA in total RNA was confirmed by a control PCR using total RNA as templates. Aliquots of 1 µg total RNA were used for first-strand cDNA synthesis using a PrimeScript RT reagent kit (DRR037S, Takara, Dalian, China) in a 20 µl reaction. In this reaction system, random primers and oligo dTs were added according to the manufacturer's instructions. Real-time PCR was performed in a 20 µl reaction using 10 µl 2× SYBR Green Premix Ex Taq II (DRR081A, Takara), 2.5 µl cDNA, and 0.2 µl of 20 mM primers (Supplementary Table S1) in an IQ5 Real Time System (Bio-Rad, Hercules, CA, USA). To ensure the primer specificity, PCR products were sequenced and aligned with homologues from *P. trichocarpa* and other model plants (Supplementary Fig. S2). *Actin217* was used as a reference gene (Brunner et al., 2004). PCR was performed in triplicate together with a dilution series of the reference gene. The efficiencies of all PCR reactions were between 95 and 105% (Supplementary Table S1).

Statistical analysis

Net flux data were calculated by Mageflux version 1.0 attached to the SIET system (Xu et al., 2006). Statistical tests were performed with Statgraphics (STN, St Louis, MO, USA). Data were tested for normality before further analysis. The effects of species and N treatment on variables were analysed by two-way ANOVAs. Differences between means were considered significant when the *P*-value of the ANOVA *F*-test was less than 0.05. The *C_q* values obtained from qPCR were normalized using the program proposed by Pfaffl et al. (2002) and the fold-changes of transcript levels were calculated in the program of REST (Pfaffl et al., 2002) as described by Li et al. (2012). For principal component analysis (PCA), data were standardized and computed by the command `prcomp()` in R (<http://www.r-project.org/>). The cluster analysis of gene expression was computed by command `heatmap.2()` with the package 'gplots' in R.

Results

Root morphology and photosynthesis

Root morphology and photosynthesis are sensitive to changes in resource (e.g. N) availability. Thus, these characteristics were analysed in both poplar species (Table 1). Pp and Pg had distinct

Table 1. Root morphological, photosynthetic characteristics, and starch of *P. popularis* (Pp) and *P. alba* × *P. glandulosa* (Pg) exposed to 10, 100, or 1000 µM NH₄⁺NO₃

Species	N treatment (µM)	Root biomass (g DW)	Total fine root length (m)	Total fine root surface area (cm ²)	Total root volume (cm ³)	A (mmol CO ₂ m ⁻² s ⁻¹)	WUE _i (mmol CO ₂ mol ⁻¹ H ₂ O)	PNUE _i (mg N ⁻¹ s ⁻¹)	Foliar starch (mg (g DW) ⁻¹)	Root starch (mg (g DW) ⁻¹)
Pp	10	4.4 ± 0.3 ^{bc}	21.9 ± 2.0 ^a	123.3 ± 14.4 ^{cd}	4.9 ± 0.0 ^a	6.8 ± 0.7 ^a	134.1 ± 26.8 ^d	1.8 ± 0.1 ^a	11.8 ± 0.1 ^b	12.3 ± 0.8 ^{ab}
	100	4.5 ± 0.3 ^c	39.9 ± 2.2 ^b	158.2 ± 18.5 ^d	4.6 ± 0.8 ^a	9.8 ± 0.3 ^b	120.7 ± 3.2 ^d	2.4 ± 0.2 ^b	11.2 ± 1.2 ^b	13.6 ± 0.2 ^b
	1000	3.5 ± 0.3 ^{abc}	19.6 ± 2.1 ^a	87.8 ± 1.8 ^{bc}	6.2 ± 0.5 ^a	17.1 ± 0.8 ^{cd}	73.7 ± 0.2 ^c	4.0 ± 0.4 ^c	8.3 ± 0.1 ^a	10.8 ± 1.1 ^a
Pg	10	2.5 ± 0.4 ^a	22.0 ± 8.5 ^a	71.2 ± 11.8 ^{ab}	5.7 ± 0.7 ^a	7.7 ± 0.4 ^a	40.9 ± 0.2 ^a	2.5 ± 0.6 ^b	14.0 ± 0.1 ^c	13.3 ± 0.2 ^b
	100	3.4 ± 0.6 ^a	11.5 ± 1.8 ^a	46.3 ± 8.4 ^a	9.2 ± 0.5 ^b	10.2 ± 0.2 ^b	45.2 ± 1.8 ^{ab}	2.8 ± 0.5 ^{bc}	10.9 ± 0.5 ^b	12.4 ± 0.4 ^{ab}
	1000	2.5 ± 0.3 ^{ab}	12.8 ± 2.2 ^a	48.9 ± 7.5 ^a	9.1 ± 0.4 ^b	14.6 ± 0.7 ^c	52.3 ± 4.0 ^b	3.3 ± 0.2 ^c	11.4 ± 0.1 ^b	12.0 ± 0.9 ^{ab}
P-values	Species	***	**	****	****	****	****	NS	**	NS
	N	NS	NS	*	**	***	NS	**	***	NS
	Species × N	NS	**	*	*	*	*	NS	*	NS

Data indicate mean ± SE (*n* = 6). Different letters in the same column indicate significant difference (*P* < 0.05). *P*-values of the ANOVAs of species, N treatment, and their interaction are indicated: **P* < 0.05; ***P* < 0.01; ****P* < 0.001; *****P* < 0.0001; ns, not significant. Pp, *Populus popularis*; Pg, *Populus alba* × *Populus glandulosa*; A, leaf net photosynthetic rate; PNUE_i, instantaneous photosynthetic N use efficiency; WUE_i, intrinsic water use efficiency.

root morphological characteristics under either the control N (1000 μM NH_4NO_3) or low N (100 and 10 μM NH_4NO_3) supply levels. Generally, Pg exhibited lower root biomass, total fine root length, and total fine root surface area, but higher root volume than Pp. Photosynthesis showed no differences between Pp and Pg under the control N level. Intrinsic water use efficiency was lower in Pg than that in Pp under the given N levels. As a stored photosynthate, foliar starch concentration was higher in Pg than those in Pp under the three N supply levels. Root starch concentration was similar in Pp and Pg.

Low N availability affected root morphology and photosynthesis in both poplar species (Table 1). Total fine root surface area increased in Pp under both low N levels, but remained unaltered in Pg. Total root volume was unchanged in Pp but decreased in Pg under the lowest N supply level compared to that under the control N supply. Photosynthesis decreased stronger in Pp than those in Pg under N-limiting conditions. PNUE_i was lower in both poplar species under limiting N supply levels in comparison with that under the control N condition. As a stored photosynthate, foliar starch concentration was higher in both species under low N levels than those under the control N level. N supply levels had no effects on root starch concentration.

These data show that limiting N levels induces distinct responses of root morphology and photosynthesis in Pp and Pg, which is probably associated with interspecific differences in N metabolism.

Net fluxes of NH_4^+ , NO_3^- , and H^+ , activities of PM H^+ -ATPases, and accumulation of NH_4^+ , NO_3^- , and NO_2^-

N uptake is the first crucial step, which may lead to distinct differences in N metabolism of Pp and Pg. Net fluxes of NH_4^+

and NO_3^- measured along the root tips of Pg displayed large variation at different positions, and maximal net influxes of NH_4^+ and NO_3^- occurred at the position of 15 mm from the root apex (Supplementary Fig. S1B). Based on these findings in Pg and previous observations in Pp (Luo *et al.*, 2013), net fluxes of NH_4^+ , NO_3^- , and H^+ were measured with greater detail at the position of 15 mm from the root apex of both species (Fig. 2).

Under control N, net NH_4^+ influx was similar in roots of Pp and Pg (Fig. 2A), but net NO_3^- influx was higher in roots of Pg than those of Pp (Fig. 2B). Under 100 μM NH_4NO_3 , Pg exhibited higher net influxes of NH_4^+ or NO_3^- than Pp (Fig. 2A, B). Since net influxes of NH_4^+ and NO_3^- are associated with H^+ fluxes (Luo *et al.*, 2013), net H^+ fluxes were also determined in Pp and Pg under the three N supply levels (Fig. 2C). The net H^+ efflux was lower in Pg than in Pp under the control N level. Net H^+ flux at the root surface is coupled with activities of PM H^+ -ATPases (Luo *et al.*, 2013). Thus, PM H^+ -ATPase activities were analysed in isolated plasma membranes of fine roots. The PM H^+ -ATPase activity was similar in Pp and Pg under the control N condition (Fig. 3).

Low N supply levels always resulted in significant decreases in net NO_3^- influxes in Pp and Pg compared to the control N condition (Fig. 2B). Both low N levels led to increased net H^+ efflux in Pg, but only the lowest N level elevated net H^+ efflux in Pp in comparison with the control N supply (Fig. 2C). In Pp, the PM H^+ -ATPase activities decreased under low N supply compared to the control N condition, whereas no such effects were found in Pg (Fig. 3).

Different uptake rates of NH_4^+ or NO_3^- at the root surface of Pg and Pp exposed to the three N levels may result in differences in NH_4^+ , NO_3^- , and NO_2^- content in plants. Therefore, these compounds were further analysed (Fig. 4

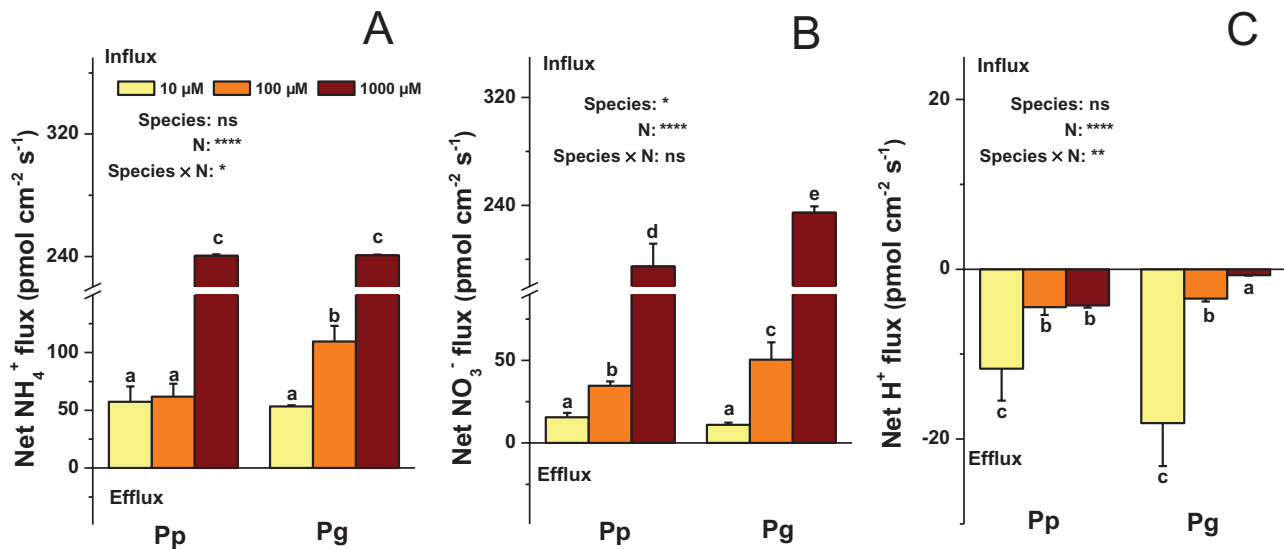


Fig. 2. Net fluxes of NH_4^+ (A), NO_3^- (B), and H^+ (C) in 10 min at 15 mm from the root apex of fine roots of *P. popularis* (Pp) and *P. alba* \times *P. glandulosa* (Pg). Data indicate mean \pm SE ($n = 6$). The measuring solution (pH 5.5) contained 0.1 mM KCl and 0.1 mM CaCl_2 as well as 10, 100, or 1000 μM NH_4NO_3 . Bars labelled with different letters indicate significant difference between the treatments. *P*-values of the ANOVAs of species, N treatment, and their interaction are indicated. * $P < 0.05$; ** $P < 0.01$; *** $P < 0.001$; **** $P < 0.0001$; ns, not significant (this figure is available in colour at JXB online).

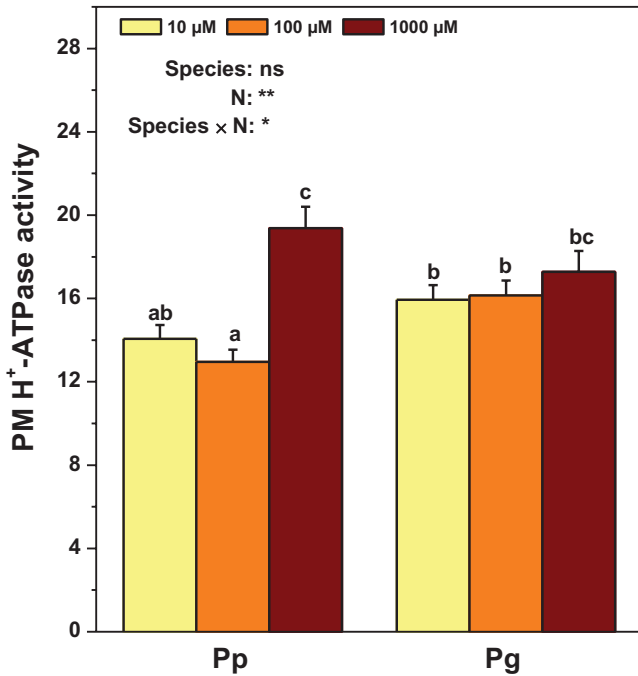


Fig. 3. PM H⁺-ATPase activity (mmol Pi h⁻¹ (mg protein)⁻¹) in roots of *P. popularis* (Pp) and *P. alba* × *P. glandulosa* (Pg) exposed to 10, 100, or 1000 µM NH₄NO₃. Bars indicate mean ± SE (*n* = 6). Different letters on the bars indicate significant difference. *P*-values of the ANOVAs of species, N treatment, and their interaction are indicated. **P* < 0.05; ***P* < 0.01; ****P* < 0.001; *****P* < 0.0001; ns, not significant (this figure is available in colour at JXB online).

and Supplementary Fig. S3). NH₄⁺ content was higher in roots of Pg than those of Pp (Fig. 4A). NO₃⁻ content was higher in roots of Pg than those of Pp under the three N levels (Fig. 4B). Root NO₂⁻ content was similar in both species (Supplementary Fig. S3). Foliar NH₄⁺ content was similar in Pp and Pg under the control N supply, but lower in Pg than in Pp under limiting N conditions (Fig. 4C). Foliar NO₃⁻ content was higher in Pg than that in Pp under the control N level (Fig. 4D).

Low N supply affected NH₄⁺, NO₃⁻, and NO₂⁻ content in poplars. In comparison with the control N level, NH₄⁺ accumulation decreased in roots of both species in response to low N supply (Fig. 4A). NO₃⁻ content increased in Pp roots under 100 µM NH₄NO₃ compared to that under the control N supply (Fig. 4B). The N treatment had no impacts on root NO₂⁻ content (Supplementary Fig. S3). Foliar NH₄⁺ content decreased in Pg in response to low N availability, but remained unaltered in Pp under the three N levels (Fig. 4C). Foliar NO₃⁻ content decreased in Pg in response to low N supply (Fig. 4D).

Activities of enzymes involved in N assimilation, total N, δ¹⁵N, and mineral nutrients

After the uptake of NH₄⁺ and NO₃⁻, enzymes play important roles in N assimilation. Therefore, this study determined the activities of enzymes (NR, NiR, GS, GOGAT, and GDH) involved in N assimilation in Pp and Pg (Figs. 5 and Supplementary Fig. S4). Root NR activity was higher in Pg

than that in Pp under the control N level (Fig. 5A). Root NiR activities were similar in Pp and Pg under the control N supply, but lower in Pg than in Pp under low N supply conditions (Supplementary Fig. S4). Root GS activity was higher in Pg than that in Pp under 100 µM NH₄NO₃ (Fig. 5B). Activities of GOGAT or GDH in roots were unaffected by species (Supplementary Fig. S4). In leaves, analysed enzyme activities of Pg were higher than those of Pp (Figs. 5C, D and Supplementary Fig. S4).

Limiting N supply also influenced activities of enzymes implicated in N assimilation in both poplar species. Root NR activity reduced in both species in response to low N levels (Fig. 5A). Root NiR activity was stimulated in Pp by 10 µM NH₄NO₃ compared with that under the control N level, but remained unchanged in Pg under the three N levels (Supplementary Fig. S4). Activities of GOGAT or GDH in roots were unaffected by low N levels (Supplementary Fig. S4). In leaves, these enzyme activities in both species remained unaltered in response to low N availability except that foliar GDH activities decreased in Pg and stimulated in Pp exposed to 10 µM NH₄NO₃ (Figs. 5C, D and Supplementary Fig. S4).

Irrespective of N forms, total N concentration in plants may mirror N availability. Moreover, fractionation of ¹⁵N may occur in different steps of N metabolism in plants, reflecting active status of N metabolism. Therefore, total N and δ¹⁵N were analysed in Pp and Pg (Fig. 6). Total N concentration in roots of Pg was higher than those of Pp under the same N level (Fig. 6A). In contrast, δ¹⁵N in roots of Pg was lower than that of Pp under the same N treatment (Fig. 6B). Foliar N concentration of Pg was also higher than those of Pp under the same N level (Fig. 6C). Foliar δ¹⁵N was unaffected by species (Fig. 6D).

Total N concentration in roots reduced with decreasing N supply levels in both species (Fig. 6A). On the contrary, δ¹⁵N in roots of both species increased in response to both low N levels (Fig. 6B). Foliar N concentration in both species was also lower under low N levels compared to those under the control N condition (Fig. 6C). In contrast, foliar δ¹⁵N in both species increased in response to low N availability (Fig. 6D).

As N availability can also affect uptake of other nutrients and carbon metabolism, mineral nutrients, soluble sugars, total C, δ¹³C, soluble protein, and phenolics were analysed in Pp and Pg (Supplementary Figs. S5 and S6, Supplementary Table S2). There were complex patterns in the responses of nutrient elements and carbon-bearing compounds to N supply levels.

PCA of morphological and physiological responses

To unravel key parameters involved in the response patterns of both poplar species to N supply levels, a PCA was conducted using data of morphological and physiological parameters related to root morphology, photosynthesis, and N metabolism (Fig. 7, Supplementary Table S3). PC1 and PC2 accounted for 37 and 20% of the variation, respectively. PC1 clearly separated the variation of species effects, and PC2 uncovered the effects of N treatment levels. Foliar N concentration and root δ¹⁵N were key contributors to PC1, whereas *A*, net influxes of NH₄⁺ and NO₃⁻, and foliar starch

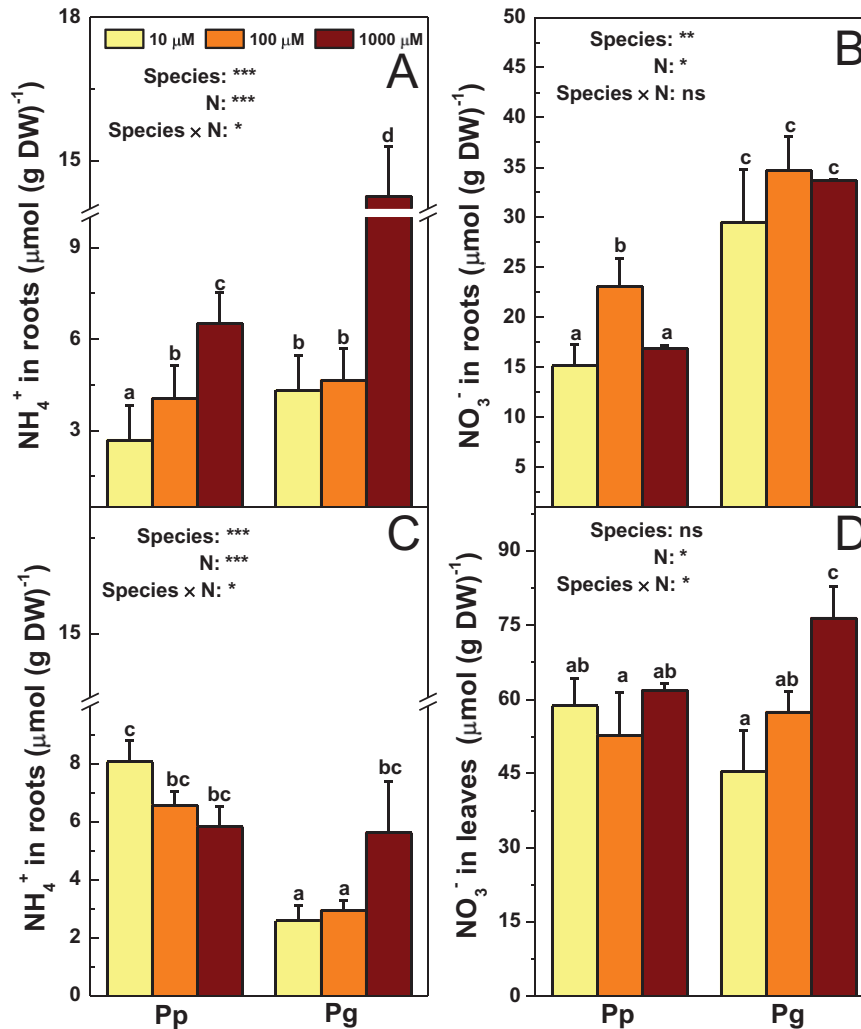


Fig. 4. NH_4^+ and NO_3^- content in roots (A and B) and leaves (C and D) of *P. popularis* (Pp) and *P. alba* × *P. glandulosa* (Pg) exposed to 10, 100, or 1000 μM NH_4NO_3 . Bars indicate mean \pm SE ($n = 6$). Different letters on the bars indicate significant difference. *P*-values of the ANOVAs of species, N treatment, and their interaction are indicated. * $P < 0.05$; ** $P < 0.01$; *** $P < 0.001$; **** $P < 0.0001$; ns, not significant. DW, dryweight (this figure is available in colour at JXB online).

concentration was important factors to PC2. In the PCA plot, a greater distance between symbols associated with N treatment levels suggests a stronger responsiveness of morphological and physiological parameters to changes in N supply levels. Thus, the greater distance between symbols related to the control N level and 100 μM NH_4NO_3 in Pp compared to that in Pg indicates that Pp is more sensitive to decreasing N supply than Pg in the range of given N availability. These PCA results indicate that Pp and Pg exhibit distinct morphological and physiological responsiveness in acclimation to limiting N availability, which mainly results from differences of Pp and Pg in uptake of NH_4^+ or NO_3^- , root ^{15}N fractionation, foliar N and starch concentration, and A.

Transcriptional regulation of genes involved in N metabolism

Since Pp and Pg demonstrated distinct patterns of morphological and physiological responses in acclimation to limiting N availability, interspecific differences may also be expected

in the transcriptional regulation pattern of key genes implicated in N metabolism. Therefore, transcript levels of representative genes involved in N acquisition and assimilation were assessed in roots and leaves of both species (Fig. 8). The cluster analysis of transcript changes of N uptake- and assimilation-related genes clearly separated Pg and Pp based on their responsiveness to N supply levels (Fig. 8).

In roots, *NRT1;2*, *NRT2;4B*, *GDH*, *NRT1;1*, and *NRT3;1C* formed a subcluster I (Fig. 8A). Under the control N level, the transcript abundance of genes in the subcluster I was higher in Pg than in Pp (Fig. 8A). The second subcluster consisted of *NRT3;1B*, *GSI;3*, *GS2*, *AMT1;2*, *VHA1;1*, and *AMT1;6* and the transcript levels of these genes were similar or lower in Pg compared to those in Pp under the control N level (Fig. 8A). The subcluster III included *NR*, *Fd-GOGAT*, *AMT2;1*, *NADH-GOGAT*, and *NiR*, and the mRNA levels of these genes were lower in Pg than those in Pp under the control N level (Fig. 8A). The strongest differences existed for *NRT2;4C* and *VHA2;2*, which were strongly suppressed in Pg compared to those in Pp under the three N supply levels (Fig. 8A).

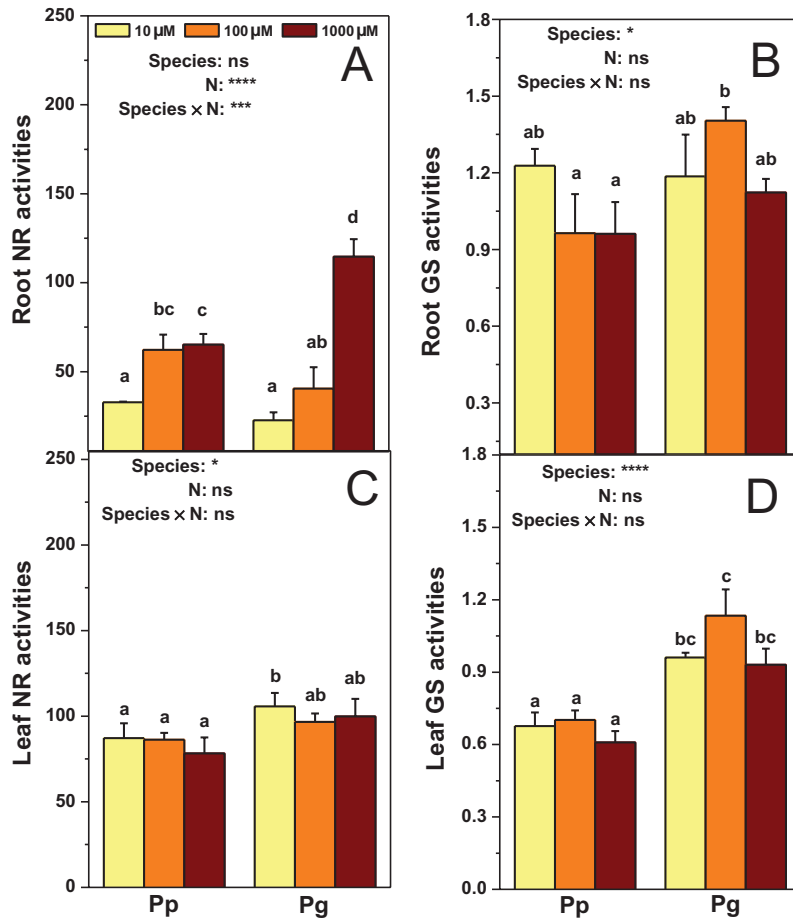


Fig. 5. Activities of nitrate reductase (NR, nmol NO₃⁻ h⁻¹ (mg protein)⁻¹), and glutamine synthetase (GS, h⁻¹ (mg protein)⁻¹) in roots (A and B) and leaves (C and D) of *P. popularis* (Pp) and *P. alba* × *P. glandulosa* (Pg) exposed to 10, 100, or 1000 μM NH₄NO₃. Bars indicate mean ± SE (*n* = 6). Different letters on the bars indicate significant difference. *P*-values of the ANOVAs of species, N treatment, and their interaction are indicated. **P* < 0.05; ***P* < 0.01; ****P* < 0.001; *****P* < 0.0001; ns, not significant (this figure is available in colour at *JXB* online).

Limiting N supply affected transcript levels of genes involved in N metabolism in roots of both species (Fig. 8A). Generally, the transcript levels of genes from the subcluster I were increased in Pp in response to low N levels in comparison with those under the control N condition, but the transcript changes of these genes in Pg were diverse in response to low N availability (Fig. 8A). The transcriptional induction of genes from subcluster II except *VHA 1;1* was detected in Pp in response to 10 μM NH₄NO₃ in comparison with those under the control N condition, but no such effects were found in Pg (Fig. 8A). The transcript levels of genes from subcluster III were suppressed in Pp in response to 100 μM NH₄NO₃ compared to those under the control N supply, but no such effects were observed in Pg (Fig. 8A). The strongest differences existed for *NRT2;4C* and *VHA2;2* because *NRT2;4C* and *VHA2;2* responded to N supply variation in Pp but not in Pg (Fig. 8A).

In leaves, *NRT3;1B*, *NiR*, *NRT2;4B*, *GDH*, and *AMT2;1* formed a subcluster I (Fig. 8B). Under the control N level, the mRNA levels of genes in the subcluster I except *AMT2;1* were higher in Pg than those in Pp (Fig. 8B). *GS2*, *NRT1;1*, *GS1;3*, and *NADH-GOGAT* constitute the second subcluster (Fig. 8B). The transcript levels of genes from this subcluster were similar

or slightly lower in Pg than those in Pp (Fig. 8B). The third subcluster consisted of *NRT3;1C*, *NRT2;4C*, *Fd-GOGAT*, and *NR* (Fig. 8B). Under the control N level, genes from subcluster III showed lower transcript levels in Pg than those in Pp (Fig. 8B). The mRNA level of *AMT1;2* was higher in Pg than that in Pp under the control N condition (Fig. 8B).

In leaves, transcript levels of genes related to N metabolism were also affected by N supply. *NRT2;4B*, *GDH*, and *AMT2;1* from subcluster I had lower transcript levels in Pp in response to low N availability compared to those exposed to the control N supply, but the transcript levels of these genes were relatively stable in Pg under the three N levels (Fig. 8B). In the second subcluster, the mRNA levels of *GS2* were stable in Pp in response to low N availability, but repressed in Pg under low N levels compared to that under the control N condition (Fig. 8B). In comparison with the control N supply, the transcript levels of genes from subcluster III were increased in Pp exposed to 10 μM NH₄NO₃, but suppressed or unaltered in Pg (Fig. 8B). The other three genes (i.e. *NRT1;2*, *AMT1;6*, and *AMT1;2*) displayed the strongest differences between Pp and Pg in response to N availability (Fig. 8B). *NRT1;2* and *AMT1;6* showed lower mRNA levels in Pp in response to low N availability, but no such effects were observed in Pg

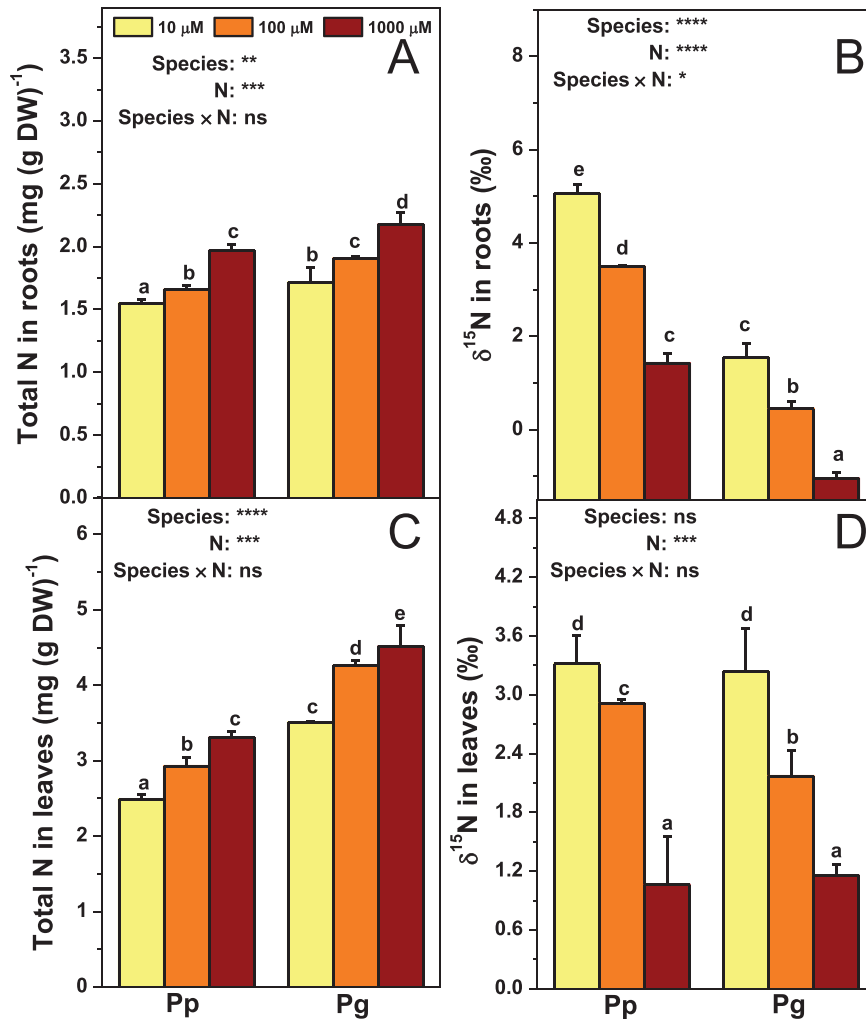


Fig. 6. Total N concentration and $\delta^{15}\text{N}$ in roots (A and B) and leaves (C and D) of *P. popularis* (Pp) and *P. alba* × *P. glandulosa* (Pg) exposed to 10, 100, or 1000 μM NH_4NO_3 . Bars indicate mean \pm SE ($n = 6$). Different letters on the bars indicate significant difference. P-values of the ANOVAs of species, N treatment, and their interaction are indicated. * $P < 0.05$; ** $P < 0.01$; *** $P < 0.001$; **** $P < 0.0001$; ns, not significant. DW, dryweight (this figure is available in colour at JXB online).

(Fig. 8B). The mRNA level of *AMT1;2* was increased in Pp but not in Pg in response to low N availability (Fig. 8B).

To find out which genes are the most important ones in response to differences in species and/or N supply levels, a PCA was performed using data of fold-changes of transcripts in Pp and Pg under the three N levels (Supplementary Table S4). PC1 clearly separated species effects and PC2 the N treatment impacts. PC1 and PC2 accounted for 48 and 26% of the variation, respectively. Leaf *NRT2;4C* and *AMT1;6*, and root *NRT2;4C* were the most important contributors to PC1, whereas *NADH-GOGAT*, *AMT1;2*, and *NRT1;2* in roots were essential factors in PC2.

Discussion

Differences between Pp and Pg in N metabolism under limiting N supply

The greater root biomass and larger fine root surface area of Pp compared with Pg suggest that root morphological

features of Pp are more responsive to limiting N availability than those of Pg. More stimulation of root growth in Pp than in Pg can be critical for different acclimation patterns of both species to limiting N availability because N acquisition in these poplars depends on root characteristics. The greater root biomass and fine root surface area in Pp indicate that Pp may better exploit nutrient resources in rhizosphere in comparison with Pg. The higher growth rates of plants may need more N metabolites to support (Lawlor, 2002). Thus, growth can be a driving force for N metabolism of plants. Consequently, the higher root growth of Pp can lead to greater N demand, further triggering a stronger responsiveness to decreasing N availability. Despite lower total N concentration in Pp roots than in Pg roots, the greater root biomass of Pp resulted in higher N amount (14–38%) in Pp roots, suggesting that Pp can acquire more N to support higher root growth.

The greater root growth in Pp, however, does not necessitate higher net influxes of N compared to those in Pg. Actually, Pp displayed lower net influxes of NH_4^+ and NO_3^- compared to those of Pg under 100 μM NH_4NO_3 , which is likely associated

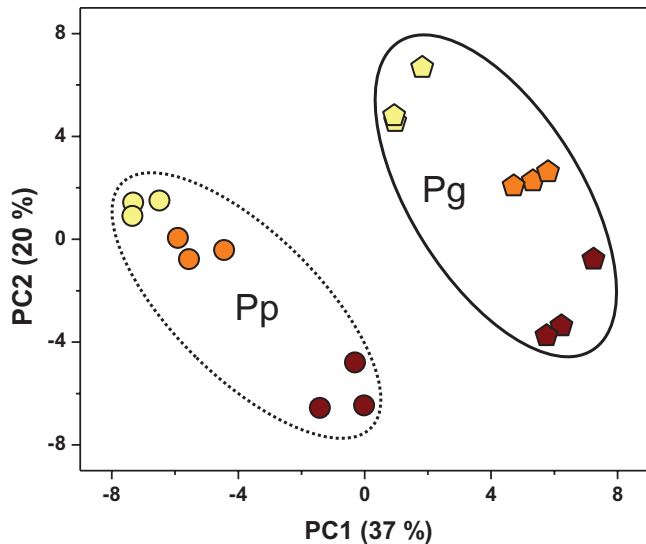


Fig. 7. Principal component analysis (PCA) plot of the first two principal components in *P. popularis* (Pp) and *P. alba* × *P. glandulosa* (Pg). The analysis was conducted using data of physiological parameters of Pp and Pg exposed to 10 (yellow), 100 (orange), or 1000 (brown) μM NH_4NO_3 , respectively (this figure is available in colour at *JXB* online).

with PM H^+ -ATPase activities, activities of enzymes implicated in N assimilation, and functioning of AMTs and NRTs (Hawkins *et al.*, 2008; Hawkins and Robbins, 2010; Alber *et al.*, 2012; Luo *et al.*, 2013). PM H^+ -ATPases play a central role in the uptake of NH_4^+ and NO_3^- because H^+ ions pumping to the apoplast through PM H^+ -ATPases create the proton motive force, driving the absorption of NH_4^+ and NO_3^- in roots (Hawkins and Robbins, 2010; Luo *et al.*, 2013). The lower activity of PM H^+ -ATPases is in line with the lower net influxes of NH_4^+ and NO_3^- in Pp compared with Pg under 100 μM NH_4NO_3 . Additionally, in most cases, the lower activities of enzymes involved in N assimilation and the lower total N concentration in roots and leaves of Pp versus Pg correspond well to the lower N uptake rates in Pp under 100 μM NH_4NO_3 . In contrast to the lower total N concentration in Pp than in Pg, the higher $\delta^{15}\text{N}$ in roots of Pp indicates that ^{15}N is more rapidly enriched in the process of N metabolism in roots of Pp than of Pg. Since the processes of N metabolism in plants discriminate against the heavier N isotope leading to the depletion of ^{15}N in plant dry mass compared with that in the soil (Tcherkez and Hodges, 2008; Falxa-Raymond *et al.*, 2012; Gauthier *et al.*, 2013), higher $\delta^{15}\text{N}$ in roots of Pp indicates less fractionation of ^{15}N occurs in Pp than in Pg. This is consistent with the lower net influxes and content of NH_4^+ and NO_3^- , activities of NR and GS, and total N concentration in Pp compared with Pg. Based on morphological and physiological parameters related to N metabolism, the PCA results suggest that Pp is more sensitive to decreasing N supply than Pg under 100–1000 μM NH_4NO_3 , which is mainly due to differences between Pp and Pg in the uptake of NH_4^+ or NO_3^- , root ^{15}N fractionation, foliar N and starch concentration, and *A*.

The distinct patterns of transcriptional regulation of genes implicated in N metabolism of Pp and Pg may be associated

with the different morphological and physiological responses of both species to limiting N availability. This study group's previous study suggests that, under N fertilization, differential expression of genes involved in N uptake (AMTs and NRTs) of Pp and Pg leads to accelerated N physiological processes in Pg than in Pp (Li *et al.*, 2012). Under limiting N conditions, however, the current data show that transcriptional regulation of key genes involved in N metabolism of Pp is more responsive than that of Pg. These results indicate that Pp and Pg can differentially manage transcriptional regulation of key genes involved in N metabolism under low and high N availability. These results are consistent with previous studies. *Arabidopsis* plants manage N metabolism differently under deficient and sufficient N conditions (Lemaitre *et al.*, 2008; Chardon *et al.*, 2010; Ikram *et al.*, 2012). These studies highlight that it is necessary to investigate the responses of plants not only to high N fertilization but also to low N availability.

Overall, Pp and Pg displayed different patterns of morphological, physiological, and transcriptional regulation in response to limiting N availability, which is mainly associated with the difference of both species in net influxes of NH_4^+ and NO_3^- , root $\delta^{15}\text{N}$, foliar N and starch concentration, *A*, and the transcriptional regulation of genes (e.g. *AMT1;2*, *NRT1;2*, and *NRT2;4C* in roots and *AMT1;6* and *NRT2;4C* in leaves) that are involved in N acquisition and assimilation.

The physiological and transcriptional regulation mechanisms of N metabolism of poplars in acclimation to low N availability

Root morphology responds highly plastic to N availability (Forde and Walch-Liu, 2009; Chapman *et al.*, 2012). Increases in fine root surface area of poplars exposed to low N levels indicate that poplars stimulate growth of fine roots to forage for nutrients under limiting N availability. Consistently, *Arabidopsis* roots adopt an 'active-foraging strategy' by outgrowth of lateral roots under limiting N conditions, but a 'dormant strategy' by inhibited growth of lateral roots under sufficient N supply (Ruffel *et al.*, 2011). Most plants can increase root growth, resulting in greater fine root surface area under short-term N deficiency, but exhibit stunted root growth under long-term limiting N availability due to lack of internal N (Kraiser *et al.*, 2011; Shen *et al.*, 2013). The current data indicate that poplar roots adopt an active-forage strategy to acquire N resources and other essential minerals under low N supply. Although poplar roots actively forage for nutrients under low N conditions, the acquired N appears insufficient for the biosynthesis of photosynthetic enzymes and metabolic precursors, leading to decreased *A* and PNUE_i. In other higher plants, N deficiency also inhibits photosynthetic capacity and growth (Sardans and Penuelas, 2012).

Gradual decreases in net influxes of NH_4^+ and NO_3^- at the root surface under decreased concentration of external NH_4NO_3 supply indicate that NH_4^+ and NO_3^- concentration in the external solution play important roles in net influxes of these ions. This was also found for seedlings of Douglas fir (*Pseudotsuga menziesii*) and soybean (*Glycine max*) (Hawkins

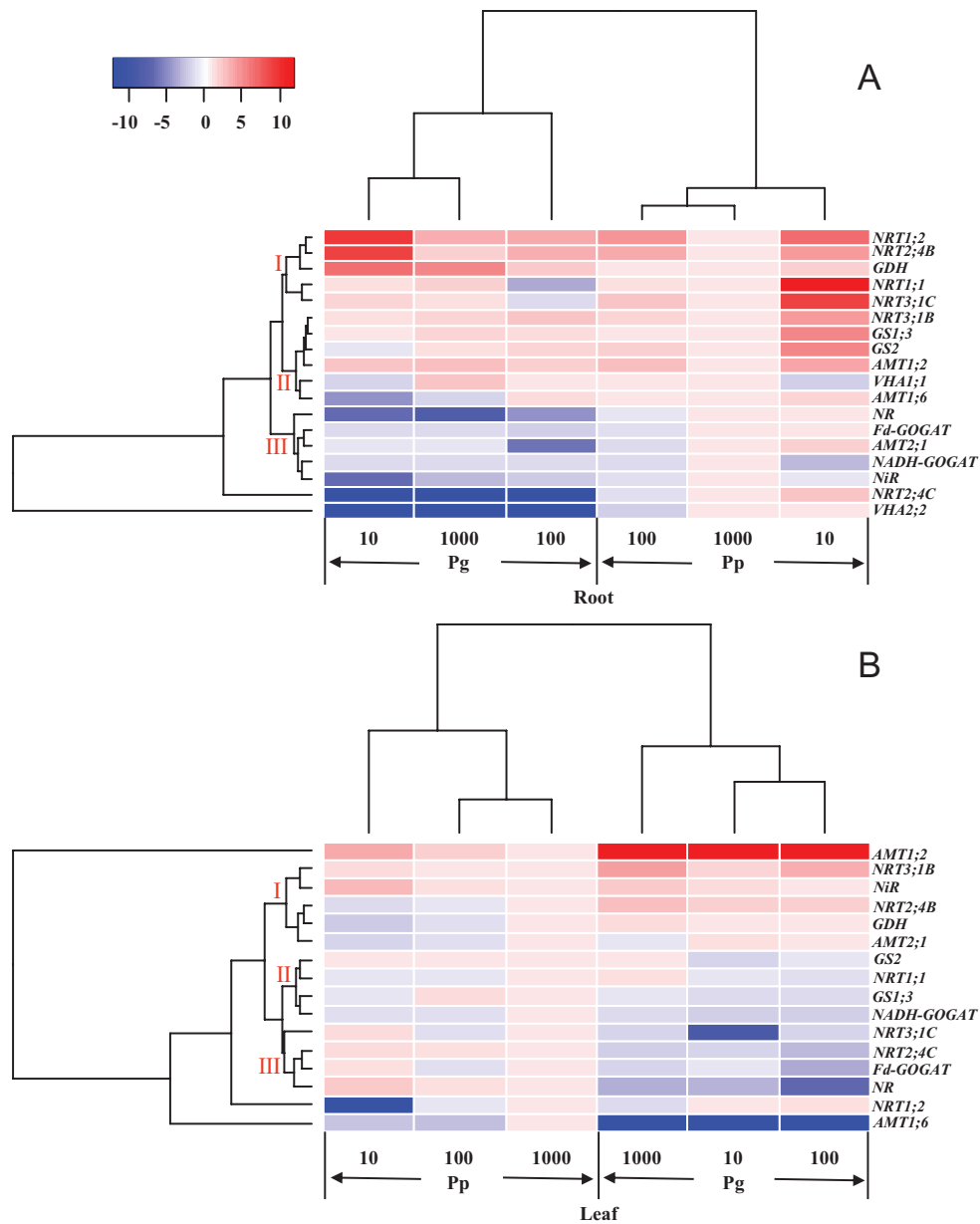


Fig. 8. Cluster analysis of transcriptional fold-changes of key genes involved in N uptake and assimilation in roots (A) and leaves (B) of *P. popularis* (Pp) and *P. alba* × *P. glandulosa* (Pg) exposed to 10, 100, or 1000 μM NH_4NO_3 . The colour scale indicates fold-changes of mRNAs. For each gene, the expression levels in roots or leaves of Pp exposed to 1000 μM NH_4NO_3 were defined as 1, and the corresponding fold-changes under 100 and 10 μM NH_4NO_3 were calculated (this figure is available in colour at *JXB* online).

and Robbins, 2010). However, net influxes of $\text{NH}_4^+/\text{NO}_3^-$ are greater at the root surface of white spruce (*Picea glauca*) exposed to 50 μM NH_4NO_3 than those of 1500 μM NH_4NO_3 (Alber *et al.*, 2012). These results suggest that impacts of external NH_4NO_3 concentration on net fluxes of $\text{NH}_4^+/\text{NO}_3^-$ are also related to plant species. Decreases in PM H^+ -ATPase activities and transcript levels of genes (*VHA1;1* and *VHA2;2*) encoding PM H^+ -ATPases, root NH_4^+ and foliar NO_3^- content, foliar GDH activity, total N concentration in roots and leaves, and soluble protein in roots and leaves of both poplar species are in agreement with lower net influxes of $\text{NH}_4^+/\text{NO}_3^-$ under limiting N supply. Moreover, correlations between different enzymes involved in N metabolism,

enzymes, gene expression levels, and transcript levels of different genes in both poplar species (Supplementary Fig. S7) indicate that poplar plants coordinate each step of N metabolism processes to acclimate to low N availability. These results indicate that the processes of N uptake and assimilation have slowed down in both poplar species in acclimation to low N availability. In plants, N and C metabolism is interconnected because the production of N metabolites such as amino acids needs C skeletons (Nunes-Nesi *et al.*, 2010). The lower total C concentration in roots and foliar $\delta^{13}\text{C}$, the elevated starch concentration in leaves, and the correlations between $\delta^{13}\text{C}$ and parameters of N metabolism in both poplar species under low N levels (Supplementary Figs. S5 and S7) suggest

that C export and/or phloem transport is inhibited under N deficiency. Foliar starch accumulation is also observed in herbaceous plants in response to low N availability, which is ascribed to the reduced demand of C skeletons for N compounds such as amino acids and proteins under low N levels (Lemaître *et al.*, 2008; Ikram *et al.*, 2012; Schluter *et al.*, 2012). In the same line, earlier studies indicate that foliar starch accumulation is a consequence of photosynthesis exceeding the demands of respiration and growth under N deficiency conditions (Lawlor *et al.*, 1987b; Lawlor, 2002).

Increases in $\delta^{15}\text{N}$ in roots and leaves of poplars under low N levels are contrary to decreases in total N concentration, indicating that ^{15}N is enriched in both poplar species under limiting N availability. N starvation also stimulates whole-plant $\delta^{15}\text{N}$ in some genotypes of wild barley (*Hordeum spontaneum*) (Robinson *et al.*, 2000). The higher $\delta^{15}\text{N}$ values in both poplar species under low N conditions compared with that under the control N supply are probably associated with slowing down of N metabolism which leads to less depletion of ^{15}N in poplars under low N availability. In other words, poplar plants are forced to utilize ^{15}N to meet their N demands under limiting N conditions, leading to ^{15}N enrichment in dry mass. Although the mechanisms underlying the variation in natural ^{15}N are not completely known in plants under various environmental conditions (Cernusak *et al.*, 2009; Tcherkez, 2011), $^{14}\text{N}/^{15}\text{N}$ fractionation can occur in the processes of N absorption, assimilation, recycling, and reallocation in plants and N release from plants (e.g. foliar NH_3 volatiles and N-containing exudates of roots; Robinson *et al.*, 2000; Ariz *et al.*, 2011; Gauthier *et al.*, 2013; Yousfi *et al.*, 2013). Additionally, changes in environmental factors such as nutrients, can cause substantial alterations in $\delta^{15}\text{N}$ in plants (Ariz *et al.*, 2011; Gauthier *et al.*, 2013; Yousfi *et al.*, 2013). Furthermore, negative correlations between $\delta^{15}\text{N}$ and transpiration rate were observed in wheat under salinity (Yousfi *et al.*, 2013). Consistently, negative correlations occur between $\delta^{15}\text{N}$ and transpiration rate, g_s , A , or PNUE_i in poplars (Supplementary Fig. S7). These results indicate that ^{15}N enrichment in poplars exposed to low N levels is probably associated with (i) less active N metabolism in poplars under low N availability and/or (ii) elevated N release from roots and leaves. The latter possibility needs further studies.

Although transcriptional regulation of genes involved in N metabolism plays a fundamental role in response to N deficiency or starvation in herbaceous plants (Hirai *et al.*, 2004; Bi *et al.*, 2007; Krouk *et al.*, 2010; Patterson *et al.*, 2010; Krapp *et al.*, 2011; Ruffel *et al.*, 2011; Engelsberger and Schulze, 2012; Kiba *et al.*, 2012; Schluter *et al.*, 2012), little is known on transcriptional regulation underlying N metabolism in trees under limiting N availability (Rennenberg *et al.*, 2009, 2010). Transcriptional induction of several *AMTs* (e.g. *AMT1;2*) and *NRTs* (e.g. *NRT1;2*, *NRT2;4B*, and *NRT3;1B*) in poplar roots exposed to low N levels indicates that poplar roots increase mRNAs of key transporters for NH_4^+ and NO_3^- as the result of acclimation to low N availability. Induced transcript abundance of *AMT1;2* is also found in roots of *P. tremula* \times *tremuloides* exposed to low N supply (Selle *et al.*, 2005) and in *P. tremula* \times *alba* under N starvation (Couturier *et al.*, 2007).

Similarly, transcription of *OsAMT1;2* in roots of rice (*Oryza sativa*) is induced by NH_4^+ deficiency (Sperandio *et al.*, 2011). *NRT2;1* (i.e., *NRT2;4C* re-defined in this study) displays higher transcript levels in NO_3^- -fed *P. \times canescens* roots than in NH_4^+ -fed roots (Ehltling *et al.*, 2007) and is induced upon application of NO_3^- to N-deprived roots of peach (*Prunus persica*) seedlings (Nakamura *et al.*, 2007). *NRT3;1* (also called *NAR2;1*) is a key player in a two-component system including *NRT2s* for nitrate transport in *Arabidopsis* (Yong *et al.*, 2010; Kotur *et al.*, 2012) and rice (Yan *et al.*, 2011). Correlation analysis between transcript levels of *NRT3;1B* or *NRT3;1C* and other *NRTs* (i.e., *NRT1;1*, *NRT2;4B*, and *NRT2;4C*) in Pp and Pg under normal and low N levels detected positive relationships (Supplementary Fig. S7). These correlations, combined with this study group's previous findings where positive correlations also occurred under N-fertilization conditions (Li *et al.*, 2012), indicate that *NRT3;1B* and/or *NRT3;1C* may also act as partners of other *NRTs* for nitrate transport in poplars under various N levels. In contrast to induction of several *AMTs* and *NRTs* in poplar roots, reduced transcript levels of most *AMTs* and *NRTs* in leaves and genes (e.g. *NR*, *NiR*, *GOGAT*) involved in N assimilation in roots and leaves of poplars indicate that N assimilation (downstream processes after N uptake) is inhibited due to shortage of N-containing precursors under low N availability. These results suggest that overexpression of *AMTs* and *NRTs* in poplar roots and downregulation of most *AMTs* and *NRTs* in leaves and genes involved in N assimilation in roots and leaves of poplars play fundamental roles in acclimation to limiting N availability.

Taken together, increased fine root growth, slowed down N acquisition and assimilation, overexpressed transcripts of *AMTs* and *NRTs* in roots, and repressed transcript levels of *AMTs* and *NRTs* in leaves and key genes involved in N assimilation are primary mechanisms of both poplar species in acclimation to limiting N availability.

In summary, Pp exhibited greater root biomass and total fine root surface area, lower net influxes of NO_3^- at the root surface, higher $\delta^{15}\text{N}$ in roots, and more responsiveness of transcriptional regulation of 18 genes involved in N uptake and assimilation in roots and leaves than Pg under limiting N supply. These results indicate that N metabolism of Pp displays a stronger responsiveness to decreasing N availability than that of Pg. Under low N conditions, decreased net influxes of NH_4^+ and NO_3^- at the root surface are consistent with lower root NH_4^+ and foliar NO_3^- content, root NR activity, total N concentration in roots and leaves, and mRNA of most *AMTs* and *NRTs* in leaves and genes involved in N assimilation in roots and leaves. Moreover, low N supply levels increased fine root surface area, foliar starch accumulation, $\delta^{15}\text{N}$ in roots and leaves, and transcript levels of several *AMTs* (e.g. *AMT1;2*) and *NRTs* (e.g. *NRT1;2*, *NRT2;4B*, and *NRT3;1B*) in roots of both poplar species. These data suggest that poplar species slow down processes of N acquisition and assimilation in acclimation to limiting N supply. These morphological, physiological, and molecular data suggest that poplar plants can differentially manage N metabolism under deficient and sufficient N conditions and that it is important to consider low N tolerance when selecting woody plants such

as *Populus* spp. for energy plantations on nutrient-poor sites. Using technologies including genomics, transcriptomics (e.g. microarray, RNA sequencing), and metabolomics in future experiments, a deeper understanding of poplars in acclimation to low N availability may be obtained.

Supplementary material

Supplementary data are available at *JXB* online.

Supplementary Table S1. Primers used for qRT-PCR.

Supplementary Table S2. Concentrations of mineral nutrients.

Supplementary Table S3. PCA of physiological parameters of both poplar species.

Supplementary Table S4. PCA of transcriptional changes of representative genes.

Supplementary Fig. S1. Net fluxes of NH_4^+ and NO_3^- along the root tip.

Supplementary Fig. S2. Alignments of representative genes.

Supplementary Fig. S3. NO_2^- content in roots and leaves.

Supplementary Fig. S4. Activities of NiR, GOGAT, and GDH in roots and leaves.

Supplementary Fig. S5. Soluble sugars, C concentration, and $\delta^{13}\text{C}$.

Supplementary Fig. S6. Soluble protein and phenolics.

Supplementary Fig. S7. Correlations of related parameters.

Acknowledgements

This work is supported by the State Key Basic Research Development Program (grant no. 2012CB416902), the National Natural Science Foundation of China (grant no. 31070539, 31100481, 31270647), the Fok Ying Tung Education Foundation (grant no. 121026), the Special Fund for Forest Science and Technology Research in the Public Interest (grant no. 201204210), and the Fundamental Research Funds for the Central Universities of China (grant no. YQ2013005). A.P. is grateful for financial support to the project BEST by the Bundesministerium für Forschung und Technologie (BMBF). The authors are grateful to C. Kettner and G. Langer-Kettner for the nutrient element analysis and R. Langel at the Center for Stable Isotopes (KOSI) of the University of Göttingen for the isotope analysis.

References

- Alber A, Ehling B, Ehling J, Hawkins BJ, Rennenberg H.** 2012. Net NH_4^+ and NO_3^- flux, and expression of NH_4^+ and NO_3^- transporters in roots of *Picea glauc.* *Trees – Structure and Function* **26**, 1403–1411.
- Ariz I, Cruz C, Moran JF, Gonzalez-Moro MB, Garcia-Olaverri C, Gonzalez-Murua C, Martins-Loucao MA, Aparicio-Tejo PM.** 2011. Depletion of the heaviest stable N isotope is associated with $\text{NH}_4^+/\text{NH}_3$ toxicity in NH_4^+ -fed plants. *BMC Plant Biology* **11**, 83
- Banziger M, Betran FJ, Lafitte HR.** 1997. Efficiency of high nitrogen environment for improving maize for low-nitrogen environment. *Crop Science* **37**, 1103–1109.
- Bi YM, Wang RL, Zhu T, Rothstein SJ.** 2007. Global transcription profiling reveals differential responses to chronic nitrogen stress and putative nitrogen regulatory components in *Arabidopsis*. *BMC Genomics* **8**, 17.
- Bilodeau-Gauthier S, Pare D, Messier C, Belanger N.** 2011. Juvenile growth of hybrid poplars on acidic boreal soil determined by environmental effects of soil preparation, vegetation control, and fertilization. *Forest Ecology and Management* **261**, 620–629.
- Black BL, Fuchigami LH, Coleman GD.** 2002. Partitioning of nitrate assimilation among leaves, stems and roots of poplar. *Tree Physiology* **22**, 717–724.
- Bradford MM.** 1976. A rapid and sensitive method for the quantification of microgram quantities of proteins utilizing the principle of protein-dye binding. *Analytical Biochemistry* **72**, 248–254.
- Brautigam A, Gagneul D, Weber AP.** 2007. High-throughput colorimetric method for the parallel assay of glyoxylic acid and ammonium in a single extract. *Analytical Biochemistry* **362**, 151–153.
- Brunner AM, Yakovlev IA, Strauss SH.** 2004. Validating internal controls for quantitative plant gene expression studies. *BMC Plant Biology* **4**, 14.
- Calfapietra C, De Angelis P, Gielen B, et al.** 2007. Increased nitrogen-use efficiency of a short-rotation poplar plantation in elevated CO_2 concentration. *Tree Physiology* **27**, 1153–1163.
- Cao X, Jia JB, Li H, Li MC, Luo J, Liang ZS, Liu TX, Liu WG, Peng CH, Luo ZB.** 2012. Photosynthesis, water use efficiency and stable carbon isotope composition are associated with anatomical properties of leaf and xylem in six poplar species. *Plant Biology* **14**, 612–620.
- Castro-Rodriguez V, Garcia-Gutierrez A, Canales J, Avila C, Kirby EG, Canovas FM.** 2011. The glutamine synthetase gene family in *Populus*. *BMC Plant Biology* **11**, 119.
- Cernusak LA, Winter K, Turner BL.** 2009. Plant $\delta^{15}\text{N}$ correlates with the transpiration efficiency of nitrogen acquisition in tropical trees. *Plant Physiology* **151**, 1667–1676.
- Chapman N, Miller AJ, Lindsey K, Whalley WR.** 2012. Roots, water, and nutrient acquisition: let's get physical. *Trends in Plant Science* **17**, 701–710.
- Chardon F, Barthelemy J, Daniel-Vedele F, Masclaux-Daubresse C.** 2010. Natural variation of nitrate uptake and nitrogen use efficiency in *Arabidopsis thaliana* cultivated with limiting and ample nitrogen supply. *Journal of Experimental Botany* **61**, 2293–2302.
- Coleman HD, Canovas FM, Man HM, Kirby EG, Mansfield SD.** 2012. Enhanced expression of glutamine synthetase (GS1a) confers altered fibre and wood chemistry in field grown hybrid poplar (*Populus tremula* × *alba*) (717-1B4). *Plant Biotechnology Journal* **10**, 883–889.
- Cooke JEK, Weih M.** 2005. Nitrogen storage and seasonal nitrogen cycling in *Populus*: bridging molecular physiology and ecophysiology. *New Phytologist* **167**, 19–30.
- Couturier J, Montanini B, Martin F, Brun A, Blaudez D, Chalot M.** 2007. The expanded family of ammonium transporters in the perennial poplar plant. *New Phytologist* **174**, 137–150.
- Dluzniewska P, Gessler A, Dietrich H, Schnitzler JP, Teuber M, Rennenberg H.** 2007. Nitrogen uptake and metabolism in *Populus* × *canescens* as affected by salinity. *New Phytologist* **173**, 279–293.

- Ehltling B, Dlugiewska P, Dietrich H, et al.** 2007. Interaction of nitrogen nutrition and salinity in grey poplar (*Populus tremula* × *alba*). *Plant, Cell and Environment* **30**, 796–811.
- Engelsberger WR, Schulze WX.** 2012. Nitrate and ammonium lead to distinct global dynamic phosphorylation patterns when resupplied to nitrogen-starved *Arabidopsis* seedlings. *The Plant Journal* **69**, 978–995.
- Euring D, Lofke C, Teichmann T, Polle A.** 2012. Nitrogen fertilization has differential effects on N allocation and lignin in two *Populus* species with contrasting ecology. *Trees – Structure and Function* **26**, 1933–1942.
- Falxa-Raymond N, Patterson AE, Schuster WSF, Griffin KL.** 2012. Oak loss increases foliar nitrogen, $\delta^{15}\text{N}$ and growth rates of *Betula lenta* in a northern temperate deciduous forest. *Tree Physiology* **32**, 1092–1101.
- Finzi AC, Norby RJ, Calfapietra C, et al.** 2007. Increases in nitrogen uptake rather than nitrogen-use efficiency support higher rates of temperate forest productivity under elevated CO_2 . *Proceedings of the National Academy of Sciences, USA* **104**, 14014–14019.
- Forde BG, Walch-Liu P.** 2009. Nitrate and glutamate as environmental cues for behavioural responses in plant roots. *Plant, Cell and Environment* **32**, 682–693.
- Gauthier PPG, Lamothe M, Mahe A, Molero G, Nogues S, Hodges M, Tcherkez G.** 2013. Metabolic origin of $\delta^{15}\text{N}$ values in nitrogenous compounds from *Brassica napus* L. leaves. *Plant, Cell and Environment* **36**, 128–137.
- Gobert A, Plassard C.** 2007. Kinetics of NO_3^- net fluxes in *Pinus pinaster*, *Rhizopogon roseolus* and their ectomycorrhizal association, as affected by the presence of NO_3^- and NH_4^+ . *Plant, Cell and Environment* **30**, 1309–1319.
- Gogstad GO, Krutnes MB.** 1982. Measurement of protein in cell suspensions using the Coomassie brilliant blue dye-binding assay. *Analytical Biochemistry* **126**, 355–359.
- Hawkins BJ, Boukcim H, Plassard C.** 2008. A comparison of ammonium, nitrate and proton net fluxes along seedling roots of Douglas-fir and lodgepole pine grown and measured with different inorganic nitrogen sources. *Plant, Cell and Environment* **31**, 278–287.
- Hawkins BJ, Robbins S.** 2010. pH affects ammonium, nitrate and proton fluxes in the apical region of conifer and soybean roots. *Physiologia Plantarum* **138**, 238–247.
- He J, Qin J, Long L, et al.** 2011. Net cadmium flux and accumulation reveal tissue-specific oxidative stress and detoxification in *Populus* × *canescens*. *Physiologia Plantarum* **143**, 50–63.
- He JL, Ma CF, Ma YL, Li H, Kang JQ, Liu TX, Polle A, Peng CH, Luo ZB.** 2013. Cadmium tolerance in six poplar species. *Environmental Science and Pollution Research* **20**, 163–174.
- Heinrichs H, Brumsack HJ, Lofffield N, Konig N.** 1986. Verbessertes Druckaufschlusssystem für biologische und anorganische Materialien. *Z Pflanzenernaehr Bodenkd* **149**, 350–353.
- Hirai MY, Yano M, Goodenowe DB, Kanaya S, Kimura T, Awazuhara M, Arita M, Fujiwara T, Saito K.** 2004. Integration of transcriptomics and metabolomics for understanding of global responses to nutritional stresses in *Arabidopsis thaliana*. *Proceedings of the National Academy of Sciences, USA* **101**, 10205–10210.
- Hirel B, Le Gouis J, Ney B, Gallais A.** 2007. The challenge of improving nitrogen use efficiency in crop plants: towards a more central role for genetic variability and quantitative genetics within integrated approaches. *Journal of Experimental Botany* **58**, 2369–2387.
- Ikram S, Bedu M, Daniel-Vedele F, Chaillou S, Chardon F.** 2012. Natural variation of *Arabidopsis* response to nitrogen availability. *Journal of Experimental Botany* **63**, 91–105.
- Jackson LE, Burger M, Cavagnaro TR.** 2008. Roots nitrogen transformations, and ecosystem services. *Annual Review of Plant Biology* **59**, 341–363.
- Johnson DW.** 2006. Progressive N limitation in forests: Review and implications for long-term responses to elevated CO_2 . *Ecology* **87**, 64–75.
- Kiba T, Feria-Bourellier AB, Lafouge F, et al.** 2012. The *Arabidopsis* nitrate transporter NRT2.4 plays a double role in roots and shoots of nitrogen-starved plants. *The Plant Cell* **24**, 245–258.
- Kotur Z, Mackenzie N, Ramesh S, Tyerman SD, Kaiser BN, Glass ADM.** 2012. Nitrate transport capacity of the *Arabidopsis thaliana* NRT2 family members and their interactions with AtNAR2.1. *New Phytologist* **194**, 724–731.
- Koyama L, Kielland K.** 2011. Plant physiological responses to hydrologically mediated changes in nitrogen supply on a boreal forest floodplain: a mechanism explaining the discrepancy in nitrogen demand and supply. *Plant and Soil* **342**, 129–139.
- Kraiser T, Gras DE, Gutierrez AG, Gonzalez B, Gutierrez RA.** 2011. A holistic view of nitrogen acquisition in plants. *Journal of Experimental Botany* **62**, 1455–1466.
- Krapp A, Berthome R, Orsel M, Mercey-Boutet S, Yu A, Castaigns L, Elftieh S, Major H, Renou JP, Daniel-Vedele F.** 2011. *Arabidopsis* roots and shoots show distinct temporal adaptation patterns toward nitrogen starvation. *Plant Physiology* **157**, 1255–1282.
- Krouk G, Mirowski P, LeCun Y, Shasha DE, Coruzzi GM.** 2010. Predictive network modeling of the high-resolution dynamic plant transcriptome in response to nitrate. *Genome Biology* **11**, R123.
- Lawlor DW.** 2002. Carbon and nitrogen assimilation in relation to yield: mechanisms are the key to understanding production systems. *Journal of Experimental Botany* **53**, 773–787.
- Lawlor DW, Boyle FA, Kendall AC, Keys AJ.** 1987a. Nitrate nutrition and temperature effects on wheat: enzyme composition, nitrate and total amino acid content of leaves. *Journal of Experimental Botany* **38**, 378–392.
- Lawlor DW, Boyle FA, Young AT, Keys AJ, Kendall AC.** 1987b. Nitrate nutrition and temperature effects on wheat: photosynthesis and photorespiration of leaves. *Journal of Experimental Botany* **38**, 393–408.
- Lawlor DW, Boyle FA, Keys AJ, Kendall AC, Young AT.** 1988. Nitrate nutrition and temperature effects on wheat: a synthesis of plant growth and nitrogen uptake in relation to metabolic and physiological processes. *Journal of Experimental Botany* **39**, 329–343.
- Lawlor DW, Kontturi M, Young AT.** 1989. Photosynthesis by flag leaves of wheat in relation to protein, ribulose biphosphate carboxylase activity and nitrogen supply. *Journal of Experimental Botany* **40**, 43–52.

- Lemaitre T, Gaufichon L, Boutet-Mercey S, Christ A, Masclaux-Daubresse C.** 2008. Enzymatic and metabolic diagnostic of nitrogen deficiency in *Arabidopsis thaliana* Wassileskija accession. *Plant and Cell Physiology* **49**, 1056–1065.
- Li H, Li MC, Luo J, et al.** 2012. N-fertilization has different effects on the growth, carbon and nitrogen physiology, and wood properties of slow- and fast-growing *Populus* species. *Journal of Experimental Botany* **63**, 6173–6185.
- Li Q, Li BH, Kronzucker HJ, Shi WM.** 2010. Root growth inhibition by NH_4^+ in *Arabidopsis* is mediated by the root tip and is linked to NH_4^+ efflux and GMPase activity. *Plant, Cell and Environment* **33**, 1529–1542.
- Lin CC, Kao CH.** 1996. Disturbed ammonium assimilation is associated with growth inhibition of roots in rice seedlings caused by NaCl. *Plant Growth Regulation* **18**, 233–238.
- Lukac M, Calfapietra C, Lagomarsino A, Loreto F.** 2010. Global climate change and tree nutrition: effects of elevated CO_2 and temperature. *Tree Physiology* **30**, 1209–1220.
- Luo J, Qin JJ, He FF, Li H, Liu TX, Polle A, Peng CH, Luo ZB.** 2013. Net fluxes of ammonium and nitrate in association with H^+ fluxes in fine roots of *Populus popularis*. *Planta* **237**, 919–931.
- Luo ZB, Calfapietra C, Liberloo M, Scarascia-Mugnozza G, Polle A.** 2006. Carbon partitioning to mobile and structural fractions in poplar wood under elevated CO_2 (EUROFACE) and N fertilization. *Global Change Biology* **12**, 272–283.
- Luo ZB, Calfapietra C, Scarascia-Mugnozza G, Liberloo M, Polle A.** 2008. Carbon-based secondary metabolites and internal nitrogen pools in *Populus nigra* under Free Air CO_2 Enrichment (FACE) and nitrogen fertilisation. *Plant and Soil* **304**, 45–57.
- Luo ZB, Polle A.** 2009. Wood composition and energy content in a poplar short rotation plantation on fertilized agricultural land in a future CO_2 atmosphere. *Global Change Biology* **15**, 38–47.
- Maizlich NA, Fritton DD, Kendall WA.** 1980. Root morphology and early development of maize at varying levels of nitrogen. *Agronomy Journal* **72**, 25–31.
- McAllister CH, Beatty PH, Good AG.** 2012. Engineering nitrogen use efficient crop plants: the current status. *Plant Biotechnology Journal* **10**, 1011–1025.
- Millard P, Grelet GA.** 2010. Nitrogen storage and remobilization by trees: ecophysiological relevance in a changing world. *Tree Physiology* **30**, 1083–1095.
- Nakamura Y, Umemiya Y, Masuda K, Inoue H, Fukumoto M.** 2007. Molecular cloning and expression analysis of cDNAs encoding a putative Nrt2 nitrate transporter from peach. *Tree Physiology* **27**, 503–510.
- Novaes E, Osorio L, Drost DR, et al.** 2009. Quantitative genetic analysis of biomass and wood chemistry of *Populus* under different nitrogen levels. *New Phytologist* **182**, 878–890.
- Nunes-Nesi A, Fernie AR, Stitt M.** 2010. Metabolic and signaling aspects underpinning the regulation of plant carbon nitrogen interactions. *Molecular Plant* **3**, 973–996.
- Ogawa T, Fukuoka H, Yano H, Ohkawa Y.** 1999. Relationships between nitrite reductase activity and genotype-dependent callus growth in rice cell cultures. *Plant Cell Reports* **18**, 576–581.
- Patterson K, Cakmak T, Cooper A, Lager I, Rasmussen AG, Escobar MA.** 2010. Distinct signalling pathways and transcriptome response signatures differentiate ammonium- and nitrate-supplied plants. *Plant, Cell and Environment* **33**, 1486–1501.
- Pfaffl MW, Horgan GW, Dempfle L.** 2002. Relative expression software tool (REST©) for group-wise comparison and statistical analysis of relative expression results in real-time PCR. *Nucleic Acids Research* **30**, e36.
- Plassard C, Guerin-Laguette A, Very AA, Casarin V, Thibaud JB.** 2002. Local measurements of nitrate and potassium fluxes along roots of maritime pine. Effects of ectomycorrhizal symbiosis. *Plant, Cell and Environment* **25**, 75–84.
- Plett D, Toubia J, Garnett T, Tester M, Kaiser BN, Baumann U.** 2010. Dichotomy in the NRT gene families of dicots and grass species. *PLoS One* **5**, e15289.
- Polle A, Douglas C.** 2010. The molecular physiology of poplars: paving the way for knowledge-based biomass production. *Plant Biology* **12**, 239–241.
- Rennenberg H, Dannenmann M, Gessler A, Kreuzwieser J, Simon J, Papen H.** 2009. Nitrogen balance in forest soils: nutritional limitation of plants under climate change stresses. *Plant Biology* **11**, 4–23.
- Rennenberg H, Wildhagen H, Ehlting B.** 2010. Nitrogen nutrition of poplar trees. *Plant Biology* **12**, 275–291.
- Robinson D, Handley LL, Scrimgeour CM, Gordon DC, Forster BP, Ellis RP.** 2000. Using stable isotope natural abundances ($\delta^{15}\text{N}$ and $\delta^{13}\text{C}$) to integrate the stress responses of wild barley (*Hordeum spontaneum* C. Koch.) genotypes. *Journal of Experimental Botany* **51**, 41–50.
- Ruffel S, Krouk G, Ristova D, Shasha D, Birnbaum KD, Coruzzi GM.** 2011. Nitrogen economics of root foraging: transitive closure of the nitrate-cytokinin relay and distinct systemic signaling for N supply vs. demand. *Proceedings of the National Academy of Sciences, USA* **108**, 18524–18529.
- Sardans J, Penuelas J.** 2012. The role of plants in the effects of global change on nutrient availability and stoichiometry in the plant–soil system. *Plant Physiology* **160**, 1741–1761.
- Schluter U, Mascher M, Colmsee C, Scholz U, Brautigam A, Fahnenstich H, Sonnewald U.** 2012. Maize source leaf adaptation to nitrogen deficiency affects not only nitrogen and carbon metabolism but also control of phosphate homeostasis. *Plant Physiology* **160**, 1384–1406.
- Selle A, Willmann M, Grunze N, Gessler A, Weiss M, Nehls U.** 2005. The high-affinity poplar ammonium importer PttAMT1.2 and its role in ectomycorrhizal symbiosis. *New Phytologist* **168**, 697–706.
- Shen JB, Li CJ, Mi GH, Li L, Yuan LX, Jiang RF, Zhang FS.** 2013. Maximizing root/rhizosphere efficiency to improve crop productivity and nutrient use efficiency in intensive agriculture of China. *Journal of Experimental Botany* **64**, 1181–1192.
- Sorgona A, Lupini A, Mercati F, Di Dio L, Sunseri F, Abenavoli MR.** 2011. Nitrate uptake along the maize primary root: an integrated physiological and molecular approach. *Plant, Cell and Environment* **34**, 1127–1140.

- Sperandio MVL, Santos LA, Bucher CA, Fernandes MS, de Souza SR.** 2011. Isoforms of plasma membrane H⁺-ATPase in rice root and shoot are differentially induced by starvation and resupply of NO₃⁻ or NH₄⁺. *Plant Science* **180**, 251–258.
- Studer MH, DeMartini JD, Davis MF, Sykes RW, Davison B, Keller M, Tuskan GA, Wyman CE.** 2011. Lignin content in natural *Populus* variants affects sugar release. *Proceedings of the National Academy of Sciences, USA* **108**, 6300–6305.
- Swain T, Goldstein JL.** 1964. The quantitative analysis of phenolic compounds. In: JB Pridham, ed, *Methods in polyphenol chemistry*. Oxford: Pergamon Press. pp 131–145.
- Tcherkez G.** 2011. Natural ¹⁵N/¹⁴N isotope composition in C₃ leaves: are enzymatic isotope effects informative for predicting the ¹⁵N-abundance in key metabolites? *Functional Plant Biology* **38**, 1–12.
- Tcherkez G, Hodges M.** 2008. How stable isotopes may help to elucidate primary nitrogen metabolism and its interaction with (photo)respiration in C₃ leaves. *Journal of Experimental Botany* **59**, 1685–1693.
- Toledo Machado A, Silvestre Fernandes M.** 2001. Participatory maize breeding for low nitrogen tolerance. *Euphytica* **122**, 567–573.
- Tuskan GA, DiFazio S, Jansson S, et al.** 2006. The genome of black cottonwood, *Populus trichocarpa* (Torr. & Gray). *Science* **313**, 1596–1604.
- Xu GH, Fan XR, Miller AJ.** 2012. Plant nitrogen assimilation and use efficiency. *Annual Review of Plant Biology* **63**, 153–182.
- Xu Y, Sun T, Yin LP.** 2006. Application of non-invasive microsensing system to simultaneously measure both H⁺ and O₂ fluxes around the pollen tube. *Journal of Integrative Plant Biology* **48**, 823–831.
- Wang L, Zhou QX, Ding LL, Sun YB.** 2008. Effect of cadmium toxicity on nitrogen metabolism in leaves of *Solanum nigrum* L. as a newly found cadmium hyperaccumulator. *Journal of Hazardous Materials* **154**, 818–825.
- Wang YY, Hsu PK, Tsay YF.** 2012. Uptake, allocation and signaling of nitrate. *Trends in Plant Science* **17**, 458–467.
- Weih M.** 2004. Intensive short rotation forestry in boreal climates: present and future perspectives. *Canadian Journal of Forest Research-Revue Canadienne De Recherche Forestiere* **34**, 1369–1378.
- Werner RA, Bruch BA, Brand WA.** 1999. ConFlo III – an interface for high precision δ¹³C and δ¹⁵N analysis with an extended dynamic range. *Rapid Communications in Mass Spectrometry* **13**, 1237–1241.
- Wilkins O, Waldron L, Nahal H, Provart NJ, Campbell MM.** 2009. Genotype and time of day shape the *Populus* drought response. *The Plant Journal* **60**, 703–715.
- Yan M, Fan XR, Feng HM, Miller AJ, Shen QR, Xu GH.** 2011. Rice OsNAR2.1 interacts with OsNRT2.1, OsNRT2.2 and OsNRT2.3a nitrate transporters to provide uptake over high and low concentration ranges. *Plant, Cell and Environment* **34**, 1360–1372.
- Yemm EW, Willis AJ.** 1954. The estimation of carbohydrates in plant extracts by anthrone. *The Biochemical Journal* **57**, 508–514.
- Yong ZH, Kotur Z, Glass ADM.** 2010. Characterization of an intact two-component high-affinity nitrate transporter from *Arabidopsis* roots. *The Plant Journal* **63**, 739–748.
- Yousfi S, Serret MD, Arous JL.** 2013. Comparative response of δ¹³C, δ¹⁸O and δ¹⁵N in durum wheat exposed to salinity at the vegetative and reproductive stages. *Plant, Cell and Environment* **36**, 1214–1227.
- Yousfi S, Serret MD, Marquez AJ, Voltas J, Arous JL.** 2012. Combined use of δ¹³C, δ¹⁸O and δ¹⁵N tracks nitrogen metabolism and genotypic adaptation of durum wheat to salinity and water deficit. *New Phytologist* **194**, 230–244.
- Zhu Y, Di T, Xu G, Chen X, Zeng H, Yan F, Shen Q.** 2009. Adaptation of plasma membrane H⁺-ATPase of rice roots to low pH as related to ammonium nutrition. *Plant, Cell and Environment* **32**, 1428–1440.